FABRICATION AND CHARACTERIZATION OF POLYMERIC NANOFIBERS AND NANOTUBES FOR CONTROLLED RELEASE OF ROSE BENGAL

Sezin Sayın

Submitted to the Graduate School of Engineering and Natural Sciencs

In partial fulfillment of the requirements for the degree of

Master of Science

Sabanci University

June 2019

TITLE OF THE THESIS/DISSERTATION

FABRICATION AND CHARACTERIZATION OF POLYMERIC NANOFIBERS AND NANOTUBES FOR CONTROLLED RELEASE OF ROSE BENGAL

APPROVED BY:

Assoc. Prof. Dr. Gözde Özaydın İnce.....
(Thesis Supervisor)

Assoc. Prof. Dr. Güllü Kızıltaş Şendur.....

Prof. Dr. Lokman Uzun.....

DATE OF APPROVAL: 20/06/2019

© Sezin Sayın 2019

All rights reserved

FABRICATION AND CHARACTERIZATION OF POLYMERIC NANOFIBERS AND NANOTUBES FOR CONTROLLED RELEASE OF ROSE BENGAL

Sezin Sayın

Master of Science Thesis, 2019

Supervisor: Assoc. Prof. Gozde Ozaydin Ince

Keywords: Initiated chemical vapor deposition, electrospinning, stimuli responsive polymeric nanotubes, stimuli responsive polymeric nanofibers, controlled release

Abstract

Advances in nanotechnology in the last decades have paved the way for significant achievements in diagnosis and treatment of various diseases. Different types of functional nanostructures have been explored and utilized as tools for addressing the challenges in detection or treatment of diseases. In particular, one-dimensional nanostructures hold great promise in biomedical applications due to their increased surface area to volume ratios, which allow better targeting, increased loading capacity and enhanced controlled delivery. Stable polymeric nanostructures that are stimuli-responsive, biocompatible and biodegradable are especially preferred for bio-applications. This thesis focuses on the fabrication and characterization of stimuli-responsive polymeric nanofibers and nanotubes for controlled delivery of Rose Bengal (RB) molecules. Single layer and coaxial polymeric nanostructures were prepared by using initiated chemical vapor deposition (iCVD) and electrospinning. iCVD technique was used for additional stimuli responsive properties such as pH, temperature and CO_2 responses. Coaxial poly(4-vinylpyridine-*co*-ethylene glycol dimethacrylate) deposited poly(vinyl alcohol)-RB blend nanofibers were synthesized for controlled RB release in medium at different pH values. Coaxial nanotubes with outer layer of polydopamine-folic acid and with inner layer of poly(methacrylic acid-co-ethylene glycol dimethacrylate) were fabricated for pH controlled and folate receptor targeted RB delivery.

Dual responsive poly(n-[3-(dimethylamino)propyl]methacrylamide-*co*-ethylene glycol dimethacrylate) nanotubes were deposited to obtain CO_2 and temperature responsive RB release. Release and loading studies from these nanostructures were performed by using UV-Vis spectroscopy. Korsmeyer-Peppas equation was employed to investigate release kinetics. It was concluded that through responsive polymer coatings, the release kinetics of the nanotubes and fibers could be controlled.

POLİMERİK NANOLİFLERİN VE NANOTÜPLERİN KONTROLLÜ ROSE BENGAL SALIMI İÇİN ÜRETİLMESİ VE KARAKTERİZASYONU

Sezin Sayın

Yüksek Lisans Tezi, 2019

Tez Danışmanı: Doç. Dr. Gozde Ozaydin Ince

Anahtar Kelimeler: Başlatıcılı kimyasal buhar biriktirme, elektroeğirme, uyarıya duyarlı polimerik nanotüpler, uyarıya duyarlı polimeric nanolifler, kontrollü salım

Özet

Son yıllarda, hastalıkların teşhisinde ve tedavisinde nanoteknoloji büyük etkiye sahip olmuştur. Bu bağlamda, farklı fonksiyonel nanoyapılar geliştirilmiş ve kullanılmıştır. Özellikle, tek-boyutlu nanoyapılar, yüksek yüzey alanı-hacim oranları vasıtasıyla hedef tedavi, yüksek ilaç yükleme kapasitesi ve geliştirilmiş kontrollü salımda umut vaat etmektedir. Uyarıya duyarlı, biyouyumlu ve biyoçözünür stabil polimerik nanoyapılar, biyo-uygulamalar için tercih edilmektedir. Bu çalışmada, uyarıya duyarlı nanolif ve nanotüp yapıları, kontrollü Rose Bengal (RB) salımı için üretilmiş ve karakterize edilmiştir. Tek katmanlı ve eşeksenli polimerik nanoyapılr, başlatıcılı kimyasal buhar biriktirme (iCVD) ve elektroeğirme metodları kullanılarak hazırlanmıştır. iCVD tekniği pH, sıcaklık ve CO_2 gibi uyarılara duyarlı özellikler eklemek için kullanılmıştır. Eşeksenli poli(4-vinylpyridine-*co*-ethylene glycol dimethacrylate) kaplanmış poli(vinyl alcohol)-RB karışım nanolifleri farklı pH değerlerine sahip ortamlarda kontrollü RB salımı için sentezlenmiştir. Polidopamin-folik asit dış katmanlı ve poli(methacrylic acid-co-ethylene glycol dimethacrylate) iç katmanlı eşeksenli nanotüpler pH kontrollü ve folat reseptör hedefli RB taşınımı için üretilmiştir. CO_2 ve sıcaklığa duyarlı poly(n-[3-(dimethylamino)propyl]methacrylamide-*co*-ethylene glycol dimethacrylate) nanotüpler ikili kontrollü RB salımı için kaplanmıştır. Bu yapılarda gerçekleşen salım ve yükleme çalışmaları UV-Vis spektroskopi kullanılarak incelenmiştir.

Salım kinetic modellerine Korsmeyer-Peppas denklemi uygulanarak bakılmıştır. Uyarıya duyarlı polimer kaplamaları ile nanotüp ve liflerin salım kinetikleri kontrol edilebilmiştir.

To AES...

ACKNOWLEDGEMENT

First, I want to thank my thesis supervisor Assoc. Prof. Gözde Özaydın İnce for her support and advices throughout my master studies. My thesis jury Assoc. Prof. Güllü Kızıltaş Şendur and Prof. Lokman Uzun for their precious comments and contributions. Prof. Selmiye Alkan Gürsel, Prof. Mehmet Ali Gülgün and Prof. Cleva Ow Yang for always having time and open doors for me.

I am also grateful to Dr. Ali Tufani for helping me at any time, for his patience and scientific assistance, Ece Özdemir and Egemen Acar for being the best teammates, Farzin Asghari Arpatappeh for his support in electrospinning, and my laboratory colleagues Mehmet Can Zeybek and Can Eğil.

I would like to thank Yonca Belce and Semih Pehlivan who made me feel at home, the best roommate Dilara Kaya, and my beloved friends Ogeday Rodop, Elif Çelik, Melike Barak, Adnan Taşdemir, Caner Dikyol and Ebru Çetin. I want to also thank Mehmet Serhat Aydın who understands me all the time, made me peaceful and who was there for me whenever I need.

Lastly, I want to thank my family Ayşe Yağcı, Esin Şentürk and Halil Şentürk for their continuous encouragement, support, patience and love. Wherever I go, they were and will always with me.

TABLE OF CONTENT

CHAPTER 1 1
INTRODUCTION 1
1.1. Drug Delivery Systems (DDS) 1
1.2. Stimuli Responsive Polymers (SRP) 2
1.3. Release Kinetics Models 4
1.4. Polymeric Nanotubes and Nanofibers in DDS 5
CHAPTER 2 14
EXPERIMENTAL PROCEDURE AND CHARACTERIZATION 14
2.1. Initiated Chemical Vapor Deposition (iCVD) 14
2.2. Electrospinning 16
2.3. Characterization 18
2.3.1. Fourier Transform Infrared Spectroscopy (FTIR) 18
2.3.2 Ellipsometry 18
2.3.3. Scanning Electron Microscopy (SEM) 19
2.3.4. Ultraviolet-visible Spectroscopy (UV-Vis) 19
CHAPTER 3 21
COAXIAL ELECTROSPUN NANOFIBERS WITH PH RESPONSIVE COATING FOR CONTROLLED DRUG DELIVERY 21
3.1. Introduction 21
3.2. Materials and Methods 24
3.3. Results and Discussion 26
3.4. Conclusion 31
CHAPTER 4 32
COAXIAL POLYMERIC NANOTUBES FOR TARGETED AND CONTROLLED DRUG DELIVERY APPLICATIONS 32
4.1. Introduction 32
4.2. Materials and Methods 33
4.3. Results and Discussion 34
4.4. Conclusion 38
CHAPTER 5 39

FABRICATION OF DUAL RESPONSIVE NANOTUBES FOR CONTROLLED RELEASE 39
5.1. Introduction 39
5.2. Materials and Methods 40
5.3. Results and Discussion 40
5.4. Conclusion 43
CONCLUSION 44
BIBLIOGRAPHY 45

LIST OF FIGURES

Figure 1. Thermo-responsive loading-release mechanism of Doxorubicin from polyglycidyl methacrylate - p(N-isopropyl acrylamide) nanotubes I) Drug Loading: nanotubes were loaded with Doxorubicin at 37°C II) Preservation: The drug is preserved inside the nanotubes at 25°C. III) Drug Releasing: The drug is released when the nanotubes are heated to 37°C. IV) Recovery: Nanotubes are cooled to their initial shape 7

Figure 2. a) Monitored tumor inoculation and growth over time. b) Measurements of tumour bioluminesce with and without nanotube application over time. c) Tumor weight change with different type of drug usage. d) Influence of nanotube method with tumor bioluminesce. e) Metastasis frequency of different parts of body 8

Figure 3. Release mechanism of ciprofloxacin loaded nanofibers due to environmental pH change. Encapsulated drug is released when the pH is adjusted to 5.2 which is lower than pKa of polymer. 10

Figure 4. Mechanism of smart hyperthermia nanofiber in response to alternating magnetic field. Doxorubicin is integrated into the chemically crosslinked nanofibers. When alternating magnetic field is turned on, magnetic nanoparticles produce enough heat to provide the activation of release mechanism of the drug. Produced heat and Doxorubicin lead to apoptosis of cancer cells 11

Figure 5. iCVD System used for 1-D nanostructure synthesis. Polymerization occurs in the anodic aluminum oxide pores conformally (left) [74] and Scanning electron microscopy imaging of stimuli responsive polymeric nanotubes synthesized by iCVD (right). 15

Figure 6. Poor step coverage in solution coated micro-trenches (left), and top, bottom and side conformal coverage of polymer by CVD 16

Figure 7. Electrospinning scheme showing grounded spinneret, high voltage power supply and fiber formation 17

Figure 8. Rose Bengal Calibration Curve 20

Figure 9. Schematic of the synthesis of the coated fiber mats. (a) Electrospinning of the PVA-RB for the fabrication of the RB loaded fiber mats. (b) Polymer coating of the electrospun fiber mats. p(4VP-co-EGDMA) is deposited on the fibers via iCVD. (c) Coaxial fiber mat of RB loaded PVA with a pH responsive polymer coating 25

Figure 10. SEM images of (a) uncoated PVA-RB nanofibers and (b) p(4VP-*co*-EGDMA) deposited PVA-RB nanofibers..... 26

Figure 11. FTIR spectra of (a) PVA nanofibers, (b) PVA-RB nanofibers, (c) p(4VP-*co*-EGDMA) coated PVA-RB nanofibers, and (d) p(4VP-*co*-EGDMA) thin film on Si wafer. The bands at 1597 and 1415 cm^{-1} corresponding to the pyridine ring vibrations (indicated with asterix) can also be observed on the coated PVA-RB nanofibers (c) confirming the presence of the polymer coating. 27

Figure 12. RB Release from (a) coated fiber mats and (b) uncoated group in PBS solutions at pH 4, pH 6.5 and pH 9. Data fitting was performed up to 60% of RB release using Korsmeyer- Peppas equation 29

Figure 13. Top and Cross-sectional images of non-etched p(MAA-*co*-EGDMA)/PDA-FA nanotubes 35

Figure 14. Top and Cross-sectional images of etched p(MAA-*co*-EGDMA)/PDA-FA nanotubes 35

Figure 15. FTIR spectra of p(MAA-*co*-EGDMA) thin films 36

Figure 16. Swelling behaviour of p(MAA-*co*-EGDMA) thin films 37

Figure 17. Release profiles from p(MAA-*co*-EGDMA)/PDA-FA nanotubes..... 38

Figure 18. SEM Images of etched p(DMAPMA-*co*-EGDMA) nanotubes 40

Figure 19. FTIR spectra of p(DMAPMA-*co*-EGDMA) thin films 41

Figure 20. Release profiles from p(DMAPMA-*co*-EGDMA) nanotubes at different gas ambient and temperatures 42

LIST OF TABLES

Table 1. Korsmeyer-Peppas Parameters and Implications 5

Table 2. Korsmeyer-Peppas parameters of release profiles..**Error! Bookmark not defined.**

Table 3. Korsmeyer-Peppas parameters of release profiles from p(MAA-*co*-EGDMA)/PDA-FA nanotubes 37

Table 4. Korsmeyer-Peppas parameters of release profiles from p(DMAPMA-*co*-EGDMA) nanotubes 42

LIST OF SYMBOLS AND ABBREVIATIONS

RB	Rose Bengal
iCVD	Initiated chemical vapor deposition
DDS	Drug delivery systems
SRP	Stimuli responsive polymers
CO_2	Carbon dioxide
f_t	Drug release fraction at time t
a	Korsmeyer-Peppas equation constant
n	Exponent of release
t	Time
AAO	Anodic aluminum oxide
FTIR	Fourier transform infrared spectroscopy
T	Thickness of swollen sample
T_0	Thickness of dry sample
SEM	Scanning electron microscopy
UV-Vis	Ultraviolet-Visible
PVA	Poly(vinyl alcohol)
p(4VP-co-EGDMA)	Poly(4-vinylpyridine-*co*-ethylene glycol dimethacrylate)
TBPO	Tertbutyl peroxide
PBS	Phosphate-buffered saline
Mt	Amount of drug released at time t
M_∞	Total amount of drug loaded
PDA	Polydopamine
FA	Folic acid
p(MAA-*co*-EGDMA)	Poly(methacrylic acid-*co*-ethyleneglycol dimethacrylate)
NaOH	Sodium hydroxide
HCl	Hydrochloric acid
p(DMAPMA-*co*-EGDMA)	Poly(n-[3-(dimethylamino)propyl]methacrylamide-*co*-ethylene glycol dimethacrylate)
N_2	Nitrogen

CHAPTER 1

INTRODUCTION

1.1. Drug Delivery Systems (DDS)

Drug delivery systems (DDS) are mainly studied to enhance therapeutic and pharmacological features of drugs. Main problems of drugs used in therapies are poor solubility, tissue damage, rapid breakdown, unfavorable pharmacokinetics, insufficient biodistribution and non-selectivity to target tissues. Potential DDS offer both hydrophilic and hydrophobic environment with enhanced drug solubility, drug release regulation, protection of drug from early degradation and ligand-mediated targeting. In this context, potency, stability, size, charge and biodistribution of drug carriers are the most important properties for DDS (Allen and Cullis, 2004). DDS propose improved drug loading and release by achieving continuous drug level maintenance with desired dosage, decreasing side effects by targeting to specified cell or tissue type, reducing needed drug amount and invasive dosage, providing short in vivo half-lives. Even though, there are many advantages of DDS as listed above, some shortcomings present due to toxicity of drug carrier material, non-convenience of system insertion and expenses (Langer, 1998).

DDS studies are improved mainly by controlling drug delivery to get sustained release. Controlled drug delivery enables improved efficacy, reduced toxicity, and desired drug dosage. In general, the purpose of DDS is to release drug molecules throughout the treatment within a time. Having high drug concentration leads to toxic effect while less amount of it

causes sub-therapeutic level. Controlled drug delivery provides the release in an extended time with therapeutic drug dosage window. Temporal and distribution-controlled systems are the main mechanisms used in controlled drug delivery. In temporal control, the aim is to extend the release duration. Responsive materials are used in this type of DDS. In distribution-controlled systems, targeting of release to the specified site is aimed. After comparison between drug concentration and side effect, optimum level is determined, and the drug delivery is adjusted accordingly. Implanting the carrier directly to the desired site, colloidal carriers as targeting agents and linkages on carriers are mainly used in distribution-controlled treatments (Uhrich et al., 1999).

Among materials used in nano-scale DDS, polymers are considerable due to their diversity in chemistry, controllable materials properties and orientation of functional groups (Goldberg et al., 2007; Coelho et al., 2010). Using the polymeric system, drugs can be delivered by three mechanisms; diffusion, enzymatic or chemical reaction with degradation of system, and solvent activation such as swelling. In general, drug is entrapped to the polymeric system and applied to the body by implantation or injection. Non-degradable polymers such as silicone capsules have been used for this type of DDS. The problem of it is less diffusion of drugs through polymers. For this reason, matrix type of system with high concentration of drug loading to the polymers in which pores present for diffusion of drug is improved. For biodegradable systems, lactic/glycolic acid copolymers have been introduced (Langer, 1998).

1.2. Stimuli Responsive Polymers (SRP)

Stimuli responsive polymers change their physical or chemical features as a response to an external stimulus such as pH, mechanical force, temperature, magnetic field, etc. These smart polymers can be used as sensors, shape-memory devices, drug delivery vehicles, and actuators (Wei et al., 2017). These polymers are fabricated from functional monomers with well-defined chemistry. Some methods used for stimuli responsive polymer fabrication are living anionic and cationic polymerization and free radical polymerization. During polymerization, SRP can be tailored by the functional groups with respect to chemical, electrical, mechanical, optical and biological properties (Gao et al., 2017).

There are two types of DDS in which SRP are utilized. Externally regulated DDS include magnetically, ultrasonically, light, thermally and electrically stimulated polymeric vehicles. Self-regulated systems comprise pH, ionic strength, enzyme, glucose and urea responsive polymers (Kost and Langer, 2012; Mura et al., 2013).

pH responsive polymers reversibly change their volume, conformation, configuration and volume with the change in external pH. The reasons behind these alterations are change in ionic and hydrophobic interactions and hydrogen bonding (Dai et al., 2008). For polymers to have pH responsive nature, they should have ionizable basic or acidic functional groups. With the pH change, these groups become protonated or deprotonated, flocculated, chain collapsed or extended, and precipitated. These states result in swelling, deswelling of polymers or formation of micelles, gels, vesicles. Polymers having carboxylic, sulfonic, phosphonic and boronic acid are some examples of pH-responsive acidic polymers. pH-responsive basic polymers are acrylates, acrylamides and vinyl containing polymers having pyrrolidine, imidazole, pyridine, piperazine, amine and morpholino groups (Kocak et al., 2017). These types of polymers are used in controlled release of drugs in cancer therapies (Schmaljohann, 2006).

Temperature responsive polymers show volume phase transition (collapsing or extension) with alteration in solvation state by heating or cooling. Polymers that become insoluble by heating have lower critical solution temperature (LCST), whereas polymers becoming soluble by heating have upper critical solution temperature (UCST). With the change in temperature, there become competing between intra-and inter-molecular hydrogen bonding and solubilization in water (Schmaljohann, 2006). Above LCST, polymer chains collapse due to domination of intramolecular hydrophobic interactions. Additionally, collapsing increases further with the intermolecular hydrophobic interactions (Crespy and Rossi, 2007).

CO_2 responsive polymers should have some functional groups such as amidines, amines and guanidines. These groups are organobases and they can react with carbonic acid that is formed by CO_2 with organic solvents and water. pH-responsive polymers should have addition of acid and base resulting in by-product. On the other hand, CO_2 responsive

polymers have no resultant contamination and they have enhanced reversibility (Liu et al., 2017).

1.3. Release Kinetics Models

During DDS studies, in vitro dissolution tests are very important with respect to describing kinetic models and release dosage (Costa and Lobo, 2001). In other words, quantitative analyzes by using different theoretical models give the DDS performance. These mathematical models are used in medicine, genetics, economy, biology and engineering technology. According to the mathematical functions, the best suitable dissolution profile is obtained, and model parameters are acquired. Curve fitting, statistical analyses and model independent methods are used for comparing model-based release profiles (Ramteke et al., 2014). Some of the most common models used for release kinetics are zero-order, first-order, Higuchi, Hixson-Crowell and Korsmeyer-Peppas.

In zero-order kinetic model, drug release from the carrier do not disaggregate and drug release is slow. Area is assumed to be constant and there is no equilibrium condition. The graph, amount of drug dissolved in time t vs time, obtained by this model is linear. It can be used in transdermal systems, matrix tablets with low soluble drugs, osmotic systems, etc. (Costa and Lobo, 2001).

First order release model is applied to absorption or elimination of drugs. It assumes solid particle dissolution in a liquid medium including surface action (Costa and Lobo, 2001). The graph of release amount of drug logarithm vs time is linear. This model is applicable to water soluble drugs in porous matrices.

Higuchi model is applied to water soluble and low soluble drugs within the solid and/or solid-like matrices. Diffusion medium is assumed to be uniform, homogeneous and planar matrix system. The model is based on square root time dependent Fick’s law (Costa and Lobo, 2001).

Hixson-Crowell model is for in plane dissolution parallel to the drug surface. Matrix is assumed to diminish with the constant initial geometry. Drug particles dissolution rate limits the release rate and diffusion from polymeric matrix has no effect (Costa and Lobo, 2001).

Korsmeyer-Peppas kinetic model is semi-empirical. The equation is expressed as:

$$f_t = at^n$$

Where a is constant related to geometry and structure of drug form, n is the exponent of release related to release mechanism and f_t is the drug release fraction (M_t/M_∞) at time t.

This model is best for mechanisms that are not-well known and/or that have more than one type release mechanisms.

Throughout this thesis, Korsmeyer-Peppas equation was used for release kinetics up to 60% of release (Costa and Lobo, 2001).

The interpretation of release exponent is given as follows (Korsmeyer et al., 1983).

Table 1. Korsmeyer-Peppas Parameters and Implications.

Release Exponent (n)	**Release Mechanism**	**Release Rate**
0.5	Fickian diffusion	$t^{-0.5}$
0.5<n<1.0	Anomalous transport	t^{n-1}
1.0	Case-II transport	Zero order release
1.0<n	Super Case-II transport	t^{n-1}

1.4. Polymeric Nanotubes and Nanofibers in DDS

There is a significant research interest in the field of nanostructures in DDS (Zelikin et al., 2016). The development of the drug delivery systems with nanostructures changed the traditional pharmaceutical systems because of their advantages such as; controlled and sustained delivery to increase the efficiency and to decrease the side effects of the drug, prevention from any chemical reactions between the drug and the system for preserving drug well, minimizing the wastage of drug for maximizing the availability at specific site for lengthened amount of time and increasing the solubility of insufficiently water soluble drugs

(Purvya and Meena, 2011; Ali and Ahmed, 2018; Singh et al., 2011). 1D drug delivery systems of stimuli responsive polymers combine the functionalities of responsive polymers with the advantages of cylindrical shapes and therefore, have attracted significant attention in the recent years (Goldberg et al., 2007; Chen et al., 2018).

Nanotubes, which have unique electronic, thermal and structural characteristics provide a promising approach for biosensing and efficient drug delivery for detection and treatment of various diseases (Purvya and Meena, 2011; Abidian et al., 2006). They can efficiently protect the drug during the delivery process against denaturation and degradation. In addition, drug loading efficiencies are higher due to their large inner volumes (Chen, 2012). High loading efficiencies of the nanotubes allow administration of lower dosages of the drug in targeting specific cancer cells, enabling the delivery of chemotherapeutic agents with definitive structural characteristics better than conventional methods (Senapati et al., 2018; Parhi et al., 2012).

Armagan et al. (Armagan and Ince, 2015) synthesized, via templated initiated chemical vapor deposition (iCVD), externally activated, pH and temperature responsive, release rate tunable and stable coaxial nanotubes with layers of poly(N-isopropylacrylamide), poly(methacrylic acid) and poly(hydroxyethyl methacrylate) to optimize and control the release of macromolecules. By changing the pH and the temperature of the environment they could tune the release rate and prolonged the release by including a hydrogel based inner layer. The release rates were calculated to be 0.089 min^{-1} and 0.13 min^{-1} for a single layer poly(methacrylic acid) and poly(N-isopropylacrylamide) nanotubes however by combining two stimuli systems, release rates ranging between 0.052 min^{-1} and 0.134 min^{-1} were obtained. The release rate of the coaxial nanotubes reached its maximum value of 48.9% when the dye loading was performed at 25° C and release at 40°C, both at pH neutral environments. It was concluded that the release percentages of the nanotubes did not reach values as high as 50% because of the hydrophilic nature of the loaded dye. Hydrophilic dye molecules entrapped in the polymer mesh of the hydrophilic nanotubes and did not contribute to loading and release processes.

Chen et al. (Chen et al., 2014) produced thermo-responsive polyglycidyl methacrylate nanotubes with inner walls functionalized by p(N-isopropyl acrylamide) for doxorubicin release where the nanotubes were cut by sonication-induced scission method for intracellular delivery (Figure 1). The reversible closing/opening gating mechanism was activated by controlling the temperature. The system allowed enhanced loading and sustained release of the drug at 37°C when the p(N-isopropyl acrylamide) was shrinked and the system preserved the doxorubicin inside at 25ºC with negligible release. As the temperature was increased to 37ºC, 67.47% of the drug was released after 11 hours.

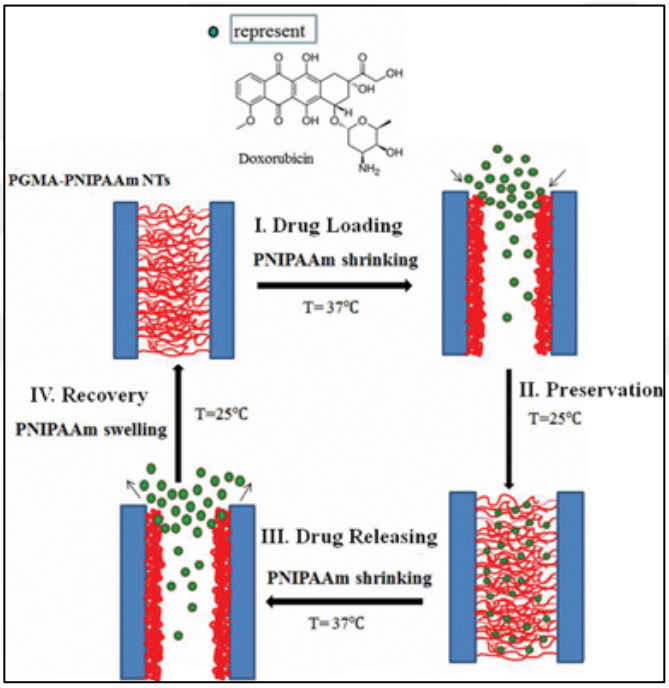

Figure 1. Thermo-responsive loading-release mechanism of Doxorubicin from polyglycidyl methacrylate - p(N-isopropyl acrylamide) nanotubes I) Drug Loading: nanotubes were loaded with Doxorubicin at 37°C II) Preservation: The drug is preserved inside the nanotubes at 25°C. III) Drug Releasing: The drug is released when the nanotubes are heated to 37°C. IV) Recovery: Nanotubes are cooled to their initial shape (Chen et al., 2014).

Newland et al. (Newland et al., 2018) synthesized cytocompatible poly ethylene glycol based soft and flexible nanotubes using the photopolymerization technique. Figure 2 shows the doxorubicin release from the nanotubes and the tumor growth analysis. At the end of the study, the equivalent quantity of doxorubicin delivered locally through the poly ethylene

glycol nanotubes showed lower tumor growth than conventional injection method. Compared to the untreated controls, tumor weight was decreased substantially from 549 ± 326 mg to 414 ± 124 mg with poly ethylene glycol nanotubes that were loaded with the "standard" dose of doxorubicin.

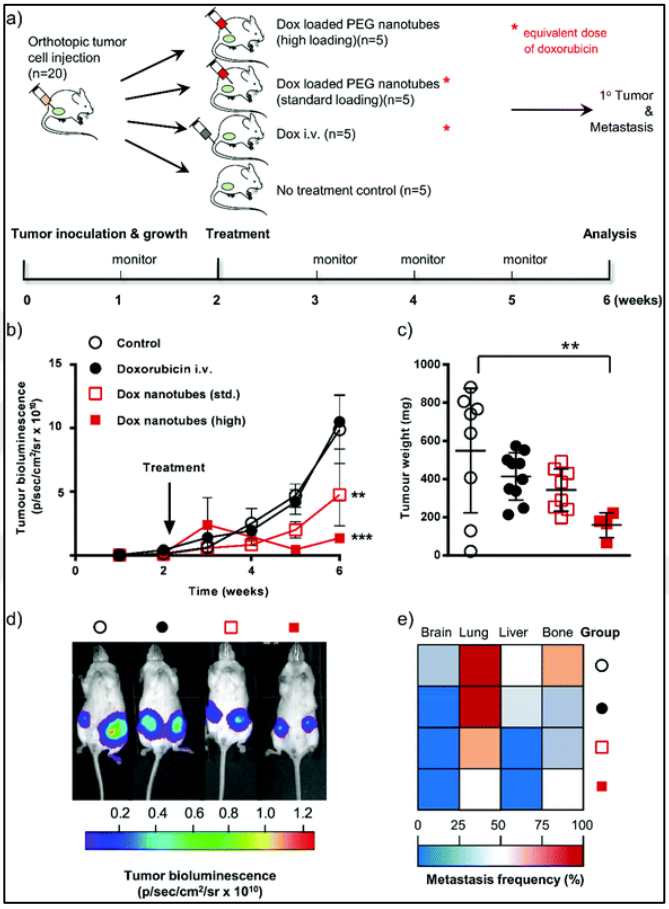

Figure 2. a) Monitored tumor inoculation and growth over time. b) Measurements of tumour bioluminesce with and without nanotube application over time. c) Tumor weight change with different type of drug usage. d) Influence of nanotube method with tumor bioluminesce. e) Metastasis frequency of different parts of body (Newland et al., 2018).

The use of nanofibers as drug carriers has also been investigated in the recent years (Al-Enizi et al., 2018; Pillay et al., 2013). As a new system for delivering ketoprofen which is a non-steroidal anti-inflammatory drug, electrospun fibers were developed (Kenawy et al., 2009). The fibers were synthesized from a biodegradable polymer, polycaprolactone, a non-biodegradable polymer, polyurethane or from the blends of the two. The results demonstrated

that the release rates of different type of fibers were comparable and the amount of drug released from fibers increased with temperature. Furthermore, the blending polycaprolactone with polyurethane, improved the mechanical properties of polycaprolactone fibers.

Mu et al. (Mu and Wu, 2017) solved the stability problem of the cancer drug cis-diamminediiodoplatinum by loading it into Poly(ε-caprolactone) nanofibers. This approach overcame the dissociation or premature interaction of drug with other molecular groups and the toxicity of the drug is highly reduced due to encapsulation by the nanofibers. Tipduangta et al. (Tipduangta et al., 2015) mixed two partially miscible polymer blends to improve the tuneability of the physicochemical and mechanical properties of the drug-loaded fibers to release two different drugs to different desired target sites. This also helped to develop controlled drug release formulations for which the release rate can be adjusted by changing the polymer ratio of the mixture.

Slemming-Adamsen et al. (Slemming-Adamsen et al., 2015) developed an easy one-step nanofiber production process which contains synthesizing and crosslinking with only electrospinning to create cross-linked poly(N-isopropylacrylamide)/gelatin electrospun nanofibers, which exhibited thermo-responsive swelling/deswelling behavior. They demonstrated the release of the encapsulated anti-cancer drug doxorubicin from the fibers, with an encapsulation efficiency of 91%, at the target temperature. Demirci et al. (Demirci et al., 2014) on the other hand, synthesized poly(4-vinylbenzoic acid-co-(ar-vinylbenzyl)trimethylammonium chloride) nanofibers via reversible addition-fragmentation chain transfer polymerization. Ciprofloxacin was encapsulated by pH-responsive nanofibers via electrospinning and the release of the drug could be controlled by adjusting the pH of the environment. The loading efficiency was calculated to be 93.4 ± 3.4%. Release studies performed at different pH conditions showed that, a 30-minute initial burst release period was followed by a sustained release period of 240 minutes in acidic medium and 480 minutes in neutral or basic media. The percentage release of the drug in the initial burst release period increased with pH because of enhanced molecular interactions (Figure 3).

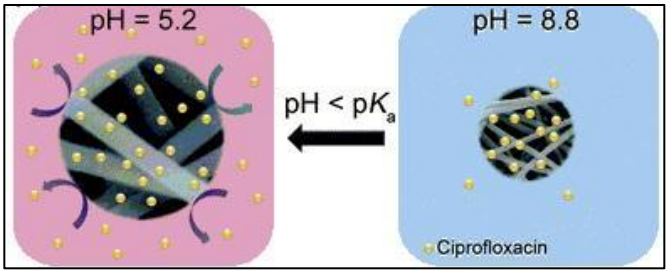

Figure 3. Release mechanism of ciprofloxacin loaded nanofibers due to environmental pH change. Encapsulated drug is released when the pH is adjusted to 5.2 which is lower than pKa of polymer (Demirci et al., 2014).

Kim et al. (Kim et al., 2013) produced smart hyperthermia nanofibers with doxorubicin and magnetic nanoparticles which generate heat and release the drug in response to an alternating magnetic field for the induction of skin cancer apoptosis. The nanofibers consisted of chemically-cross-linkable temperature-responsive polymer, magnetic nanoparticles and the drug. Magnetic nanoparticles acted as a trigger for the release of drugs. It was observed from the anticancer effect tests that 70% of human melanoma cells died in only 5 min of alternating magnetic field application to loaded nanofibers. In addition, chemically crosslinked nanofiber mesh facilitated a switchable change in the drug release ratio in response to the generated heat from the alternating magnetic field stimulation of magnetic nanoparticles, which induces the deswelling of the nanofiber (Figure 4).

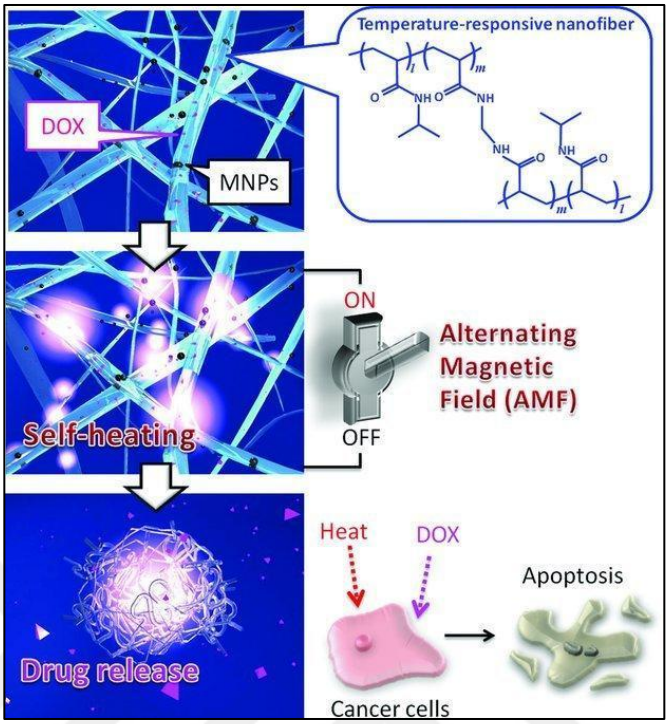

Figure 4. Mechanism of smart hyperthermia nanofiber in response to alternating magnetic field. Doxorubicin is integrated into the chemically crosslinked nanofibers. When alternating magnetic field is turned on, magnetic nanoparticles produce enough heat to provide the activation of release mechanism of the drug. Produced heat and Doxorubicin lead to apoptosis of cancer cells (Kim et al., 2013).

Through functionalization of the nanofiber surfaces, utilization of these nanostructures as drug delivery devices can be enhanced due to the additional functionalities the nanofibers attain.

Nanofiber surfaces can be easily functionalized by chemical or physical vapor deposition methods to change the chemical or mechanical properties of the surfaces (Yu et al., 2009). For hierarchical materials design, the ability to coat the surfaces of the nanofibers with polymer films is important, as the coatings can extend the range of material properties available, such as surface wettability. Superhydrophobic surfaces with a water contact angle of more than 150° can be achieved by coating submicron electrospun fiber mats with hydrophobic polymer poly(perfluoroalkyl ethyl methacrylate) with iCVD (Baxamusa et al., 2009).

Piras et al. (Piras et al., 2008) synthesized bioerodible poly(maleic anhydride-alt-2-methoxyethyl vinyl ether) by electrospinning for anti-inflammatory drug, diclofenac sodium, and human serum albumin release. They showed that separate loading of these two components resulted in uniform distribution of fibers, whereas simultaneous loading caused heterogeneous distribution. By the erosion of polymeric nanocarriers, complete release of agents was achieved within 7 hours.

Nanofibers in which some agents and structures are embedded are also used for drug delivery to improve the release kinetics. Mickova et al. (Mickova et al., 2012) embedded liposomes into coaxial polyvinyl alcohol /poly-ε-caprolactone nanofibers to enhance the short half-life, low stability and ineffective retention of liposomes. Coaxial electrospun fibers with embedded liposomes improved the release kinetics of the drug compared to the delivery systems without the liposomes. The fluorescence spectroscopy analysis showed that drug release was extended by adding liposomes to the coaxial nanofibers. The sample without the liposomes had an intense initial burst release (60.6%) that was subsequently followed by a slow release. On the other hand, the nanofibers with liposomes had a release profile which started with a lower initial burst release (20%) followed by a sustained release. The release halftime of the first sample was 20 h and for the second sample it was 112 h.

In another study, Wang et al. (Wang et al., 2010) developed a novel system for controlled drug delivery of multiple drugs using chitosan nanoparticles/polycaprolactone composite fibers, achieving the release of rhodamine B and naproxen. Drug loaded polymeric nanoparticles were embedded in the core part of the polycaprolactone fibers forming chainlike structure. The release of multiple drugs was successfully achieved by these core/shell nanofibers. It was seen that both with rhodamine B and naproxen, a controlled release was achieved when compared to conventional drug release. The cumulative drug release of Naproxen was 60.5% and was %18.1 for rhodamine-b after 72 h.

Meng et al. (Meng et al., 2011) fabricated fenbufen loaded bare poly(lactic-co-glycolic acid) and poly(lactic-co-glycolic acid)/gelatin nanofibers by electrospinning. Increasing the gelatin concentration increased the hydrophilicity of the composite material leading to the burst release of drug from the fibers. In addition, crosslinking ratio of these fibers affected

the initial burst release and with the change of the pH value of the buffer solution the release rate of fenbufen changed. Besides, the physical characteristics of fibers changed with different pH values. At higher pH, fibers switched to a rubberier state and at lower pH, fibers shifted to a glassy state more. This physical characteristic confirmed that the diffusion of the drug changed with different mobilities of distinct fiber states, leading to pH dependent release profile.

CHAPTER 2

EXPERIMENTAL PROCEDURE AND CHARACTERIZATION

This thesis focuses on the stimuli responsive polymeric nanofibers and nanotubes for controlled Rose Bengal (RB) release. To prepare these structures, versatile techniques initiated chemical vapor deposition and electrospinning were utilized. To characterize these carriers and to investigate release kinetics, Fourier transform infrared spectroscopy, liquid cell ellipsometry, scanning electron microscope and UV-Vis spectroscopy were used.

2.1. Initiated Chemical Vapor Deposition (iCVD)

Functional, responsive and biocompatible are fabricated by initiated chemical vapor deposition (iCVD). iCVD uses the advantages of CVD method to coat surfaces with polymers conformally, without the use of any solvents and enabling to tune the film properties. Reaction of initiating radicals with precursor monomers through free radical mechanism is the main principle of the iCVD polymerization (Baxamusa et al., 2009; Alf et al., 2010; Armagan and Ince, 2015) (Figure 5). The initiator and monomer precursor molecules, which are in the vapor phase, are introduced into the polymerization chamber where the radical molecules are formed via thermal of light-activated decomposition of the initiator. Conformality control is especially crucial for the synthesis of 1D nanostructures within the pores of sacrificial templates (Figure 6), and delivery of the precursors to the surface in the vapor phase provides homogeneous distribution of precursor molecules on the surface (Alf et al., 2010; Armagan and Ince, 2015; Ozaydin-Ince et al., 2011).

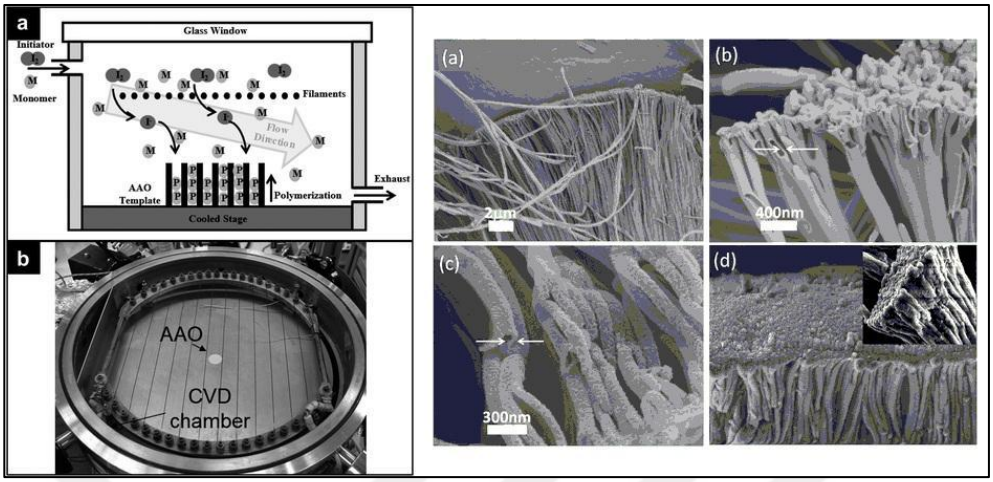

Figure 5. iCVD System used for 1-D nanostructure synthesis. Polymerization occurs in the anodic aluminum oxide pores conformally (left) [74] and Scanning electron microscopy imaging of stimuli responsive polymeric nanotubes synthesized by iCVD (right) (Armagan and Ince, 2015).

Systematic studies on the conformality of the coatings on high aspect ratio surfaces show that the surface monomer concentration and the monomer reactivity are the main factors that affect conformality (Ozaydin-Ince and Gleason, 2010). The degree of conformality, therefore, can be controlled by tuning the deposition parameters. For the synthesis of polymeric nanotubes via iCVD, sacrificial membranes with track etch pores are used. Deposition of polymer on the pore walls, followed by template etching reveals the nanotubes. Ability to control surface concentrations of the precursors separately, enables to tune the chemical composition and crosslinking density of the nanotubes (Ince et al., 2010).

The low process temperatures and operating pressures protect the functional groups of the monomer precursors, enabling synthesis of functional and stimuli responsive nanotubes (Ince et al., 2010). Through thickness control, multilayer 1D nanostructures can also be fabricated by subsequent coating of pores with different polymers.

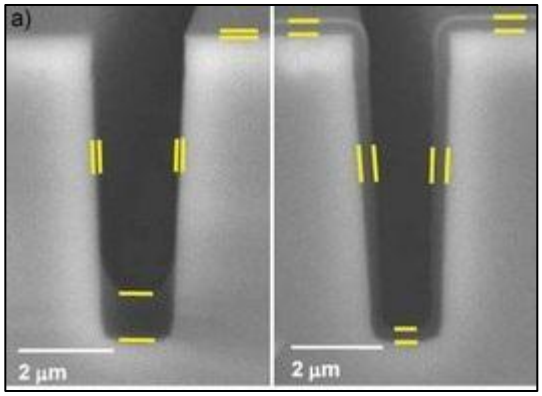

Figure 6. Poor step coverage in solution coated micro-trenches (left), and top, bottom and side conformal coverage of polymer by CVD (Alf et al., 2010).

Ozaydin-Ince et al. (Ozaydin-Ince et al., 2011) fabricated coaxial shape-memory polymeric nanotubes via templated iCVD method using anodic aluminum oxide (AAO) sacrificial templates. The coaxial nanotubes were synthesized by the subsequent coating of the template inner walls with different functional polymers. The shape memory response of the outer polymer layer was activated by the swelling of the inner hydrogel layer. The nanotubes were then used for the burst release of the cargo molecules. Armagan et al. (Armagan and Ince, 2015) reported synthesis of stimuli responsive coaxial nanotubes via iCVD (Figure 5). Each layer was a different functional polymer, responsive to different stimuli, which enabled the control of the release kinetics. The response of each layer could be controlled separately by tuning the chemical composition of the polymer layers.

2.2. Electrospinning

Electrospinning is a versatile technique to synthesize polymeric nanofibers. As shown in Figure 7, the principle is based on a grounded spinneret connected to high voltage power supply (Wallace et al., 2012). Electrostatic repulsion occurs by the application of high voltage to the spinneret tip. Polymer solution is transferred to spinneret via syringe pump. Surface tension causes pendant droplets at first and with enough voltage Taylor cone shape is obtained, resulting in the jet formation directed towards the collector. As the solvent in the solution evaporates on the collector, and polymer nanofibers are obtained on the collectors. These collectors can be copper, aluminum plates or rotating drums.

In electrospinning, polymers that can be used for fiber synthesis are limited. The disadvantage of electrospinning is that non-conducting polymers or additives should be used in the conductive polymer fiber formation. These additives decrease the conductivity but results in fine fibers (Long et al., 2011). On the other hand, with respect to other approaches, electrospinning is very useful in mass-production for continuous long nanofibers. Additionally, porosity, surface area, fiber diameter, thickness and brittleness can be adjusted for desired product shape (Long et al., 2011; Al-Enizi, et al., 2018; Schiffman and Schauer, 2008; Hrib et al., 2015). Mortar grinding, ultrasonication, razor blade cutting, and cryogenic cutting are methods forming short nanofibers (Chen et al., 2018).

Morphology of nanofibers produced by electrospinning depends on the type of the polymer and the solution properties. Polymer properties that affect the fiber morphologies are mainly molecular weight distribution, solubility, and glass-transition temperature. Among solution properties, viscosity, solution concentration, surface tension and conductivity are significant factors that affect the fiber formation. Some other parameters as substrate type, polymer feed rate, electrode geometries, humidity and field strength are also effective (Schiffman and Schauer, 2008).

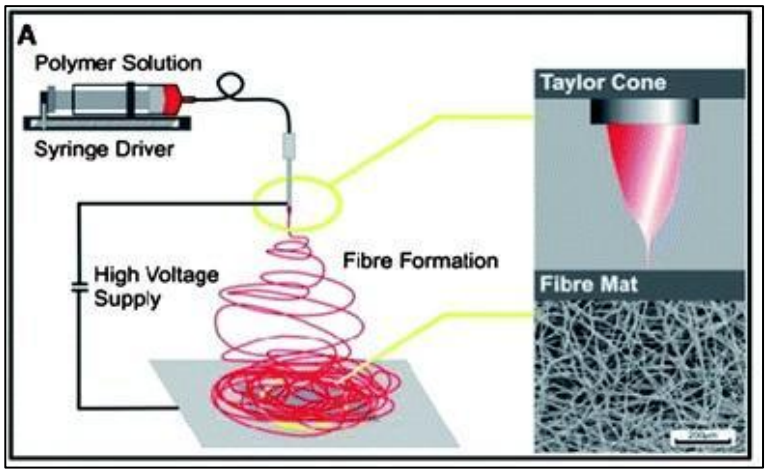

Figure 7. Electrospinning scheme showing grounded spinneret, high voltage power supply and fiber formation (Wallace et al., 2012).

For core-shell structures, coaxial electrospinning is utilized. In core-shell nanofibers, external layer, shell, usually consists of active agents specified for functionality such as

immobilized enzymes, whereas inner core layer provides mechanical support or consists of the cargo molecules in delivery applications (Khajavi and Abbasipour, 2012). Specifically, in biological applications, biomolecules are embedded in the nanofibers as the inner core. Two different solutions in the coaxial nanofiber fabrication process prevents the interaction between aqueous based organic molecules and the solvents in the polymer solution. The fiber diameter is determined by the solution concentration of the shell.

Polyvinylpyrrolidone (Tipduangta et al., 2015), polycaprolactone (Hrib et al., 2015; Kenawy et al., 2009; Yoshimoto et al., 2003; Mu and Wu, 2017), polyurethane (Kenawy et al., 2009), polylactide (Hrib et al., 2015; Kenawy et al., 2002), poly(DL,Lactide-co-glycolide) (Shin et al., 2006), polyvinyl alcohol (Hrib et al., 2015), polyvinylcaprolactam (González and Frey, 2017), chitosan (Ohkawa et al., 2004), polyaniline and polyacrylonitrile (Zhu et al., 2007) are main polymers fabricated by electrospinning that are used in biomedical applications.

2.3. Characterization

2.3.1. Fourier Transform Infrared Spectroscopy (FTIR)

Thermo-Fisher Scientific, Nicolet iS10 FTIR was used to characterize the chemical composition of prepared samples. Deposited Si wafer, bare Si wafer, coated and uncoated fibers were characterized by this method. Data were acquired with 62 scans and the resolution of 4 cm^{-1} over the range of 800-4000 cm^{-1}. During the measurements, N_2 gas was applied to the system for removing air and having smooth spectra. To obtain polymeric structures FTIR, bare Si wafer spectra was subtracted from the coated Si wafer spectra.

2.3.2 Ellipsometry

The working principle of ellipsometry is reflection of polarized lights from sample leading to angle and amplitude change. A simple ellipsometer consists of polarizer, light source and detector. During characterizations, M2000D J.A. Woollam Co. Inc. model ellipsometer was used. For swelling behavior investigations, liquid cell stage with temperature controller was used. Thickness measurements were performed at 75° nominal angle of incidence with wavelength range of 315-718 nm for 30 minutes. Data fitting was performed by using Cauchy model. During swelling investigations, liquid medium with different pH values at 4,

6.5, and 9 were utilized. Swelling percentages were calculated by using the formula $((T-T_0)*100/T_0)$, where T is the thickness of the swollen and T_0 is the thickness of the dry samples.

2.3.3. Scanning Electron Microscopy (SEM)

To characterize the morphology of fibers and nanotubes, Field Emission SEM (Zeiss, Leo Supra VP 35) was used. Fiber diameters were measured. Top and cross-sectional images of nanotubes were obtained. Samples were placed on the SEM stubs by carbon tape. They were, then, sputtered by Au-Pd by Denton Vacuum sputtering equipment for 135 seconds. Acceleration voltage was 4kV and working distance was between 6 and 8 mm.

2.3.4. Ultraviolet-visible Spectroscopy (UV-Vis)

For loading and release studies, Thermo Scientific NanoDrop 2000c UV-Vis mode was used. In each measurement, 2 µL of sample was applied. The absorbance peak of Rose Bengal is at 550 nm. First, calibration curve was drawn according to the absorbance values of the Rose Bengal solutions with known concentrations as shown in Figure 8. Then, concentration of release data was obtained by the calibration curve. The equation is $y=0.1104x+0.0012$ where x represents absorbance and y corresponds to concentration in mg/ml.

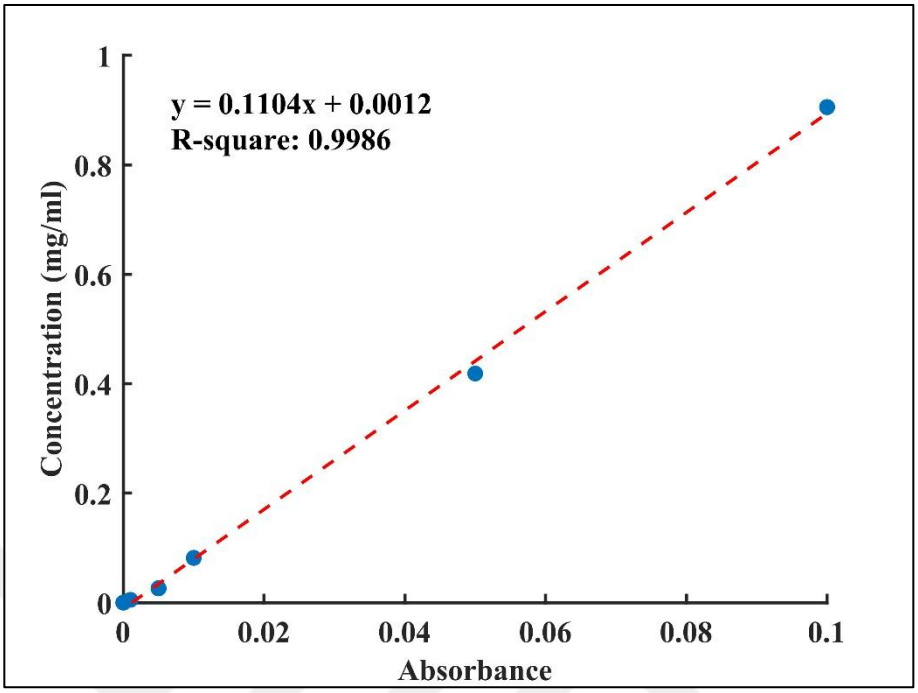

Figure 8. Rose Bengal Calibration Curve.

CHAPTER 3

COAXIAL ELECTROSPUN NANOFIBERS WITH PH RESPONSIVE COATING FOR CONTROLLED DRUG DELIVERY

3.1. Introduction

One of the scopes of this thesis was achieving controlled drug delivery with sustained release. To begin with, closed cylindrical structures with higher surface area should be employed. For this reason, fiber structures were chosen for the first study. They can be blended with the water-soluble model drug molecules and easily worked for drug delivery applications.

Implantable patches for drug delivery have gained attention in recent years. In particular, these patches are used in site-specific, targeted delivery with enhanced sustained release of drug molecules from biodegradable materials (LaPorte et al., 2005; Brown and Crawford, 2002). These devices have been developed to overcome the common challenges in drug delivery such as achieving systematic delivery with therapeutically effective drug concentrations at the specified target. Theeuwes and Nelson (Theeuwes and Nelson, 2004) developed a bilayered, patch-based device, which provided drug delivery directly to the organ surface. The biocompatible, drug-impermeable first layer acted as the drug-reservoir, while the drug-permeable second layer allowed drug delivery directly to the organ. Nelson et al. (Nelson et al., 2003), on the other hand, introduced a biodegradable fiber implant for drug release, which involved three dimensional matrices of predefined non-homogeneous patterned polymeric fibers.

Electrospun nanofibers as polymeric nanocarriers are widely used in drug delivery systems (DDS) because they have high loading and encapsulation efficiency and they can be easily produced in a cost-effective manner (Wang et al., 2010; Chakraborty et al., 2009). Blending a polymer solution with a therapeutic agent before electrospinning is the most common technique for encapsulation. The distribution of drug molecules and morphology of fibers are the main factors affecting the release behavior (Zamani et al., 2013; Kenawy et al., 2002; Tipduangta et al., 2015).

Sharma et al. (Sharma et al., 2013) loaded insulin to poly(vinyl alcohol) (PVA) and sodium alginate nanofiber-based patch for anti-diabetic drug delivery. In vivo test of the patch on male Wistar rats showed that the drug molecules were released in their pharmacologically active states without any deterioration. In another study, for the treatment of glaucoma disease, Garg et al. (Garg et al., 2014) used PVA and polycaprolactone fiber mats loaded with timolol maleate and dorzolamide hydrochloride as model drugs, achieving a very high drug entrapment efficiency of approximately 100%.

Although electrospun fibers are very promising with respect to drug delivery, in post-operation cancer treatment applications, controlling the initial burst release and tuning the release kinetics from fibers are the main challenges yet to be overcome (Thakkar and Misra, 2017).

To defeat these challenges during cancer treatments, coaxial nanofibers with core-shell structures have been introduced due to their effectiveness in drug incorporation into nanofibers as reservoir-type drug delivery carriers (He et al., 2006). Recent studies include concentric spinneret electrospinning method for coaxial nanofiber formation. These core-shell nanocarriers are used mostly to control the sustained drug delivery (He et al., 2006; Zupančič et al., 2016), to release both hydrophilic and hydrophobic drugs from the same system (Oliveira et al., 2015), to enhance implant osseointegration and to prevent implant infections (Song et al., 2013), and to obtain bi-component, surface-modified, and functional graded nanofibers (Zhang et al., 2004). Another method which has been used to overcome these shortcomings is direct deposition onto nanofibers to produce coaxial structures (Chunder et al., 2007). Layer-by-layer deposition (Sakai et al., 2009; Li et al., 2012; Croisier

et al., 2014), and vapor phase methods such as chemical vapor deposition (Zeng et al., 2005) are some examples.

Although, studies reported have included controlled drug release from various polymeric nanofibers, stimuli responsive and crosslinked coatings on these nanofibers have not been quite examined. In this paper, fabrication of polymeric mat with an outer coating layer for sustained release of a model dye was reported. PVA polymer with Rose Bengal (RB) dye solution was electrospun to form blend fibers.

PVA is used as the polymer matrix due to its biocompatibility and biodegradable nature leading to its wide utilization in drug delivery applications (Kenawy et al., 2007; Huang and Rhim, 1993; Bazhban et al., 2013; Jalvandi et al., 2017; Taepaiboon et al., 2006; Jannesari et al., 2011; Li et al., 2013; Yang et al., 2007). Meanwhile, RB (4,5,6,7-tetrachloro-2',4',5',7'-tetraiodofluoresceindisodium) is used as the model drug which is a water soluble, photosensitive, synthetic dye used for diagnostics exhibiting cytotoxicity in various cancer types such as colorectal cancer cells (Qin et al., 2017); melanoma and breast cancer cells (Toomey et al., 2013); and ovarian and adenovirus-transformed embryonic kidney cancer cells (Koevary, 2012).

In order to provide additional functionalities to the electrospun fibers, surface of the fiber mats was coated with poly(4-vinylpyridine-*co*-ethylene glycol dimethacrylate) (p(4VP-co-EGDMA)), a pH sensitive polymer, via initiated chemical vapor deposition (iCVD). iCVD is an all-dry, free-radical polymerization method which allows polymerization directly on the substrate surface, initiated by thermally decomposed radicals reacting with the monomer molecules adsorbed on the substrate (Lau and Gleason, 2006; Ozaydin-Ince et al., 2011). It is advantageous because of its conformal coating ability on high aspect ratio surfaces, which preserves the film thickness throughout the surface topography (Ozaydin-Ince et al., 2011; Armagan and Ozaydin Ince, 2015).

In the study reported here, RB release from the coaxial nanofibers is investigated at different pH values and the effect of the pH responsive polymer coating on the release performance is studied.

3.2. Materials and Methods

Materials

PVA (MW 85,000-124,000, 87-89% hydrolyzed, Aldrich), and Rose Bengal sodium salt (dye content ~90%, Aldrich) were used in electrospinning for fiber synthesis. The monomer 4VP (95%, Aldrich), the crosslinker EGDMA (98%, Aldrich), and the initiator tertbutyl peroxide (TBPO, 98%, Aldrich) were used without purification. Phosphate-buffered saline (PBS, Aldrich) was utilized for release studies.

Preparation of Fiber Mats

10 wt% PVA solution was obtained by dissolving PVA in distilled water at 70°C and stirred continuously for 4 hours. Homogeneous solution was observed after stirring at room temperature, 500 rpm overnight. PVA-RB solution was prepared by blending 100 mg/ml RB distilled water and 10 wt.% PVA solutions in RB:PVA 1:5 ratio.

Electrospinning setup includes syringe pump, stainless steel spinneret needle, high voltage supply, 10cmx10cm collector, and 2 ml syringe. The distance between needle and collector was kept 15 cm, and the voltage was applied at 8 kV. Flow rates for both PVA and PVA-RB blend solutions were adjusted as 0.3 ml/h.

Deposition of Fiber Mats

P(4VP-*co*-EGDMA) was conformally deposited on both sides of fiber mats at a thickness of 500 nm by using iCVD technique. The crosslinker EGDMA was heated to 95°C in a metal jar, and 4VP was kept at room temperature. Base pressure and base temperature for the deposition system were 1 mTorr and 46°C, respectively. The initiator was delivered to the system with the flow rate of 1.03 sccm while the flow rate of N_2 gas was 1.1 sccm. The filament and substrate temperatures were at 240°C and 25°C, respectively, throughout the deposition. Reaction pressure was fixed at 600 mTorr. Flow rates of 4VP and EGDMA were 2.73 sccm and 0.14 sccm, respectively. Si wafers were coated simultaneously as the fiber mats, to be used in ellipsometric swelling experiments. Figure 9 shows the schematic of the coated and uncoated nanofiber mat fabrication process.

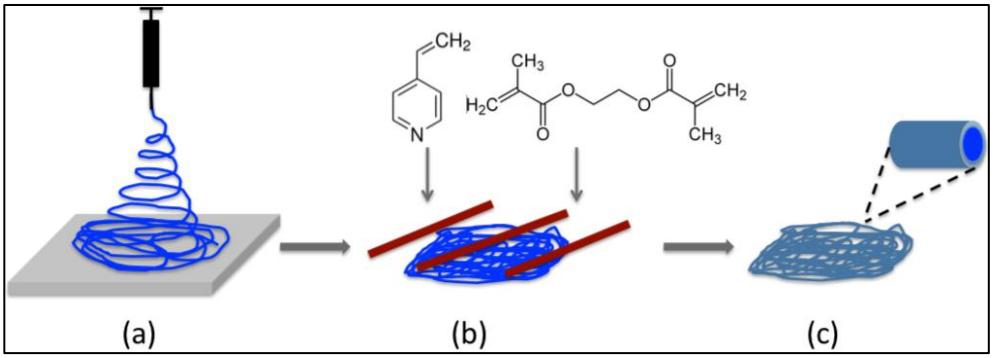

Figure 9. Schematic of the synthesis of the coated fiber mats. (a) Electrospinning of the PVA-RB for the fabrication of the RB loaded fiber mats. (b) Polymer coating of the electrospun fiber mats. p(4VP-co-EGDMA) is deposited on the fibers via iCVD. (c) Coaxial fiber mat of RB loaded PVA with a pH responsive polymer coating.

Characterization of Fibers

The structure of coated and uncoated fibers was imaged by Field emission scanning electron microscopy (Zeiss, Leo Supra VP35) with accelerating voltage of 4 kV. Uncoated and deposited nanofibers were characterized by Fourier transform infrared spectroscopy (Thermo-Fisher Scientific, Nicolet iS10 FTIR) with 62 scans and the resolution of 4 cm^{-1} over the range of 800-4000 cm^{-1}. Swelling behavior of deposited polymer film on Si wafer was investigated via spectroscopic ellipsometer (M2000D J.A. Woollam Co. Inc.) in a liquid cell stage at room temperature. Dynamic thickness measurements were performed at 75° nominal angle of incidence with wavelength range of 315-718 nm for 30 minutes. Swelling percentages were calculated by using the formula $((t-t_0)*100/t_0)$, where t is the thickness of the swollen and t_0 is the thickness of the dry samples.

Release Studies from Fibers

Coated and uncoated electrospun fibers were cut into 1 cm x 2 cm pieces and put in 10 ml PBS solutions separately at pH 4, 6.5, 9 and put on a shaker during the data acquisition to obtain homogeneity throughout the release medium. UV-Vis measurements were performed using NanoDrop UV-Vis spectrophotometer (Thermo Scientific NanoDrop 2000c). For each measurement, 100 µl of PBS solution was used and replaced with fresh PBS solution in the

release medium. For RB detection, the UV absorbance peak at 550 nm was used. The loading capacity of the fibers was determined by completely dissolving uncoated fibers and measuring the RB concentration of the solution. Release percentages of the coated fibers were obtained by dividing the concentration of RB released from the fibers by the loading capacity.

3.3. Results and Discussion

SEM images of (a) uncoated PVA-RB nanofibers and (b) p(4VP-*co*-EGDMA) coated PVA-RB nanofibers are shown in Figure 10. The average diameter of pure PVA nanofibers is approximately 425 ± 22 nm, whereas RB blended PVA nanofibers are 523 ± 39 nm in diameter. Increased concentration in solution with RB addition resulted in larger diameters observed (Aljehani et al., 2014). The iCVD polymer coating on the fibers increased the average diameter to 587 ± 63 nm, confirming that the thickness of the polymer coating is approximately 65 ± 5 nm.As confirmed by the SEM images, the structures of the fibers were not damaged after the iCVD process and the fibers could be conformally coated with the polymer layer, enabling the fabrication of coaxial p(4VP-*co*-EGDMA)-PVA-RB nanofibers.

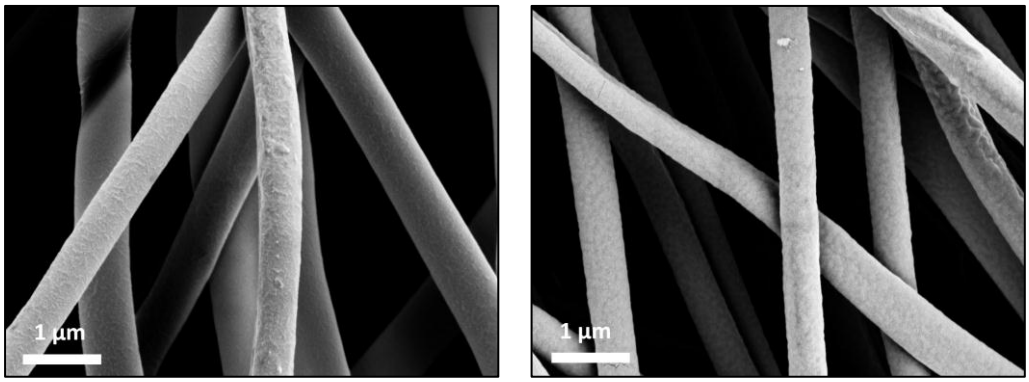

(a) (b)

Figure 10. SEM images of (a) uncoated PVA-RB nanofibers and (b) p(4VP-*co*-EGDMA) deposited PVA-RB nanofibers.

Swelling percentage of p(4VP-*co*-EGDMA) thin films on Si wafers was determined to be 62±10% at pH 4, whereas at both pH 6.5 and pH 9, swelling was less than 5%, confirming the pH response of the polymer coating. Swelling of the polymer at low pH values is

attributed to the protonation of 4VP in the acidic environment causing the chains to stretch due to electrostatic repulsion. Deprotonation of the polymer chains at high pH values, on the other hand, leads to the collapsed state observed (Li et al., 2008, Wang et al., 2013).

FTIR spectra of pure PVA, PVA-RB and p(4VP-*co*-EGDMA) coated PVA-RB nanofibers are shown in Fig.11.

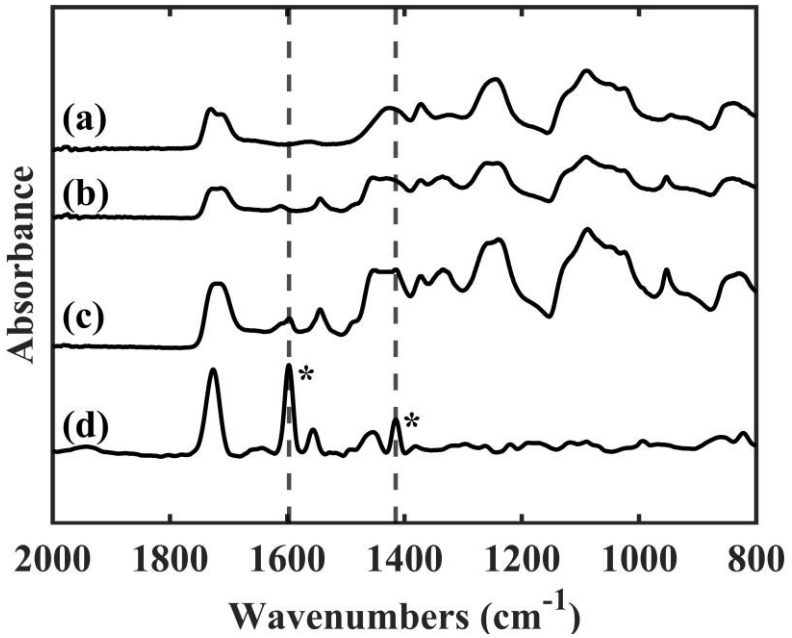

Figure 11. FTIR spectra of (a) PVA nanofibers, (b) PVA-RB nanofibers, (c) p(4VP-*co*-EGDMA) coated PVA-RB nanofibers, and (d) p(4VP-*co*-EGDMA) thin film on Si wafer. The bands at 1597 and 1415 cm^{-1} corresponding to the pyridine ring vibrations (indicated with asterix) can also be observed on the coated PVA-RB nanofibers (c) confirming the presence of the polymer coating.

The absorption bands at 1734 cm^{-1},1429 cm^{-1} and 1091 cm^{-1} are related to C=O double bond, CH_2, and C-O-C stretching modes of pure PVA nanofibers, respectively (Fig11a) (Mansur et al., 2008). The bands at 1717 cm^{-1}, 1457 cm^{-1}, 1091cm^{-1} belong to C=O double bond, CH_2, and C-O-C stretching modes of PVA for RB-PVA nanofibers. Additional bands in RB-PVA blend nanofibers at 1615 cm^{-1} belongs to C=O double bond of carbonyl group whereas at 1547, 1444, 1337 cm^{-1} corresponds to C=C double bonds of aromatic rings (Fig11b)

(Dabrzalska et al., 2016). The absorption band in coated PVA-RB nanofibers at 1719 cm^{-1} indicates CO double bond stretching of EGDMA, whereas 1599 cm^{-1}, 1547 cm^{-1}, 1417 cm^{-1} belong to pyridine ring vibration and 1060 cm^{-1} of 4VP and 954 cm^{-1} indicate in-plane and out-of-plane CH bending of 4VP (Fig11c) (Lau and Gleason, 2007; Bayari and Yurdakul, 2000), confirming the presence of the polymer coatings on the nanofibers.

RB release from the polymer coated and uncoated PVA-RB nanofibers were investigated in PBS solution at pH 4, pH 6.5, and pH 9 (Fig 12). Release experiments from the uncoated fibers showed that more than 80% of the RB was released in 1 hour with no significant dependence of the release rate on the pH of the medium (Fig. 12 (a)).

The kinetics of the RB release from the coated fibers, on the other hand, was strongly affected by the pH of the medium (Fig. 12(b)). At all pH values, the overall release was less than 60% at the end of 1 hour, indicating slower early time kinetics due to the coating layer on the fibers. As the pH decreased, slower release kinetics was observed and the overall release percentages at the end of the experiments were lower at low pH. While 98% of the RB was released at the end of 6 hours at pH 9, only 55% was released in 6 hours at pH 4.

The fast release rates and higher release percentages of RB obtained at pH 9 compared to the release rates at lower pH values can be attributed to smaller diameters of the fibers due to the collapsed state of the polymer coating, which leads to the increased free volume in the electrospun mat, resulting in improved release rates. At lower pH conditions, on the other hand, the swollen polymer coating of the nanofibers reduces the free volume in the mat and entraps the RB molecules, decreasing the overall release percentages and release rates. The prolonged release observed is, thus, caused by the longer paths the RB molecules have to diffuse through due to swollen polymer.

In addition to the changes in the free volume, the electrostatic interactions between the polymer coating and the released RB molecules may also contribute to the pH dependence of the release profiles at early times. Protonation of pyridine groups of p(4VP), which has a pKa in the rage 4.5- 4.7, occurs at lower pH values leading to an electrostatic interaction between the protonated pyridine groups and the RB molecules. This attractive interaction also contributes to the reduced release percentages observed at pH 4.

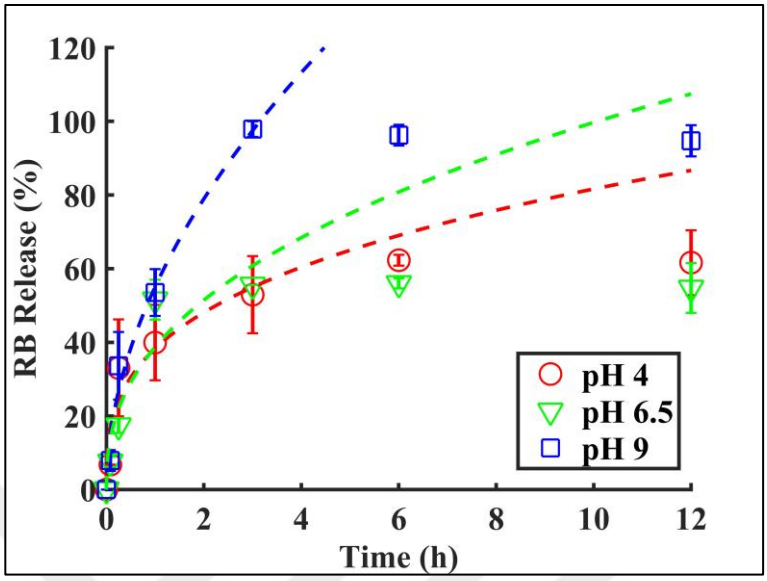

(a)

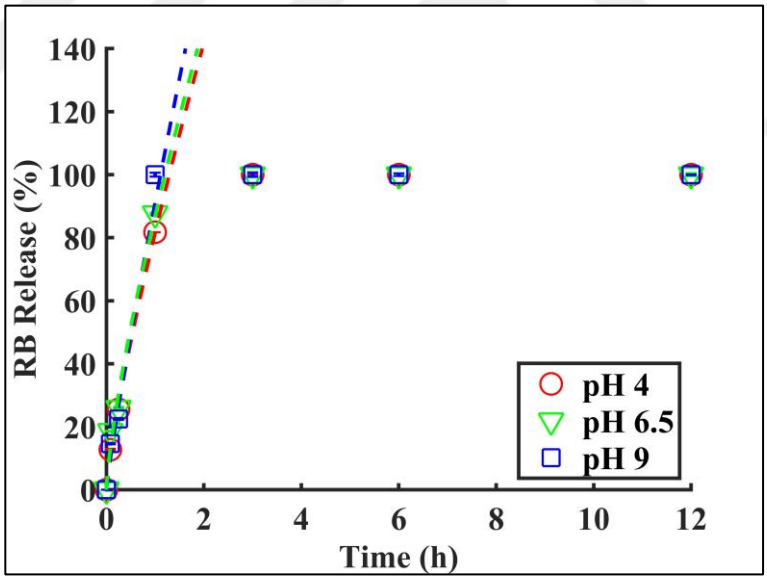

(b)

Figure 12. RB Release from (a) coated fiber mats and (b) uncoated group in PBS solutions at pH 4, pH 6.5 and pH 9. Data fitting was performed up to 60% of RB release using Korsmeyer- Peppas equation.

A transient behavior is observed at pH 6.5 with a faster early time release kinetics due to the collapsed polymer coating on the fibers, resulting in larger free space and shorter diffusion

lengths for the dye molecules. However, overall release percentages at the end of 12 hours are comparable to the release percentages at pH 4, but lower than the values obtained at pH 9.

The early time release kinetics of the polymer coated and uncoated PVA-RB nanofibers were investigated using the semi-empirical Peppas model, which includes relaxation and phase changes of the polymer matrix in addition to the diffusion of the drug molecules. The Peppas model in its simplest form is given by (Korsmeyer et al., 1983):

$$\frac{M_t}{M_\infty} = at^n \qquad \text{(Eq. 1)}$$

where M_t is the amount of drug released at time t, M_∞ is total amount of drug loaded, "a" is a constant which depends on the structure and geometry of the of drug-polymer system and "n" is the coefficient related to the mechanism of drug release (Zamani et al., 2010; Nguyen et al., 2012; Gencturk et al., 2017). The dashed lines in Fig. 4 show the fits of Eq. 1 to the early time data below 60%. The "a" and "n" values and the error R^2 obtained from the fits are given in Table 2.

Table 2. Korsmeyer-Peppas parameters of release profiles.

	coated samples			**uncoated samples**		
	R^2	n	a	R^2	n	a
pH 4	0.9096	0.3288	0.3829	0.9986	0.7991	0.8151
pH 6.5	0.9044	0.4110	0.3870	0.9876	0.7589	0.8693
pH 9	0.9461	0.5206	0.5503	0.9979	0.7655	0.7758

The control experiments performed using the uncoated fiber mats reveal a fast release kinetics at early times, which is not affected by the pH of the medium. The kinetic parameter "n" is found to be approximately 0.77 which indicates an anomalous transport mechanism, dominated by concentration dependent diffusion and dissolution of the polymer. The release kinetics from the polymer-coated samples, on the other hand, reveals a pH dependent behavior. At all pH conditions, the values of "n" are less than the control samples indicating

that the Fickian diffusion dominates over the polymer dissolution mechanism in the coated samples (Fu and Kao, 2010). As the pH of the release medium increases, faster kinetics is observed as indicated by higher "n" values. Faster kinetics at high pH values can be attributed to the collapsed state of the coating, which leads to larger free volumes compared to low pH conditions.

Although Korsmeyer-Peppas model was used to fit the release data, it should be noted that the fit parameters obtained were mostly used to study the effect of the pH on the release kinetics and to comment on the dominant mechanisms, as opposed to thoroughly explaining the active mechanisms. Our system deviates from these models due to presence of an insoluble, pH responsive polymer coating on the top and bottom layers of the mat. This coating impedes the full dissolution of the polymer fibers, introduces electrostatic interactions and impacts the diffusion paths in the swollen state, thus affecting the release rate of the drug.

3.4. Conclusion

A pH responsive coaxial fiber mat loaded with RB was produced as a potential controlled drug delivery system for post operational cancer treatments. A thin layer of pH responsive crosslinked p(4VP-*co*-EGDMA) polymer was coated on PVA-RB blend nanofibers to attain pH response to the fibers and to tune the release kinetics. The vapor-based iCVD technique was successfully employed for the conformal deposition of the polymer coating without damaging the fiber mat. The coating layer enabled to control the release kinetics of the coaxial fiber mats by tuning the pH of the medium. The iCVD was demonstrated to be a successful technique to coat fibers with stimuli responsive, functional polymer films to attain additional properties to the fibers.

CHAPTER 4

COAXIAL POLYMERIC NANOTUBES FOR TARGETED AND CONTROLLED DRUG DELIVERY APPLICATIONS

4.1. Introduction

Controlling drug delivery with nanostructures cannot be only employed with controlling drug release kinetics but also with targeting. After having controlled release from deposited fibers, targeting was studied. For this purpose, stimuli responsive hollow polymeric cylindrical structures were chosen because they have the ability of drug intake with the functional outer surface. In this part of this thesis, coaxial nanotubes were prepared with targeting outer shell and pH responsive inner layer.

Traditional anti-cancer pharmaceuticals cannot make any discrimination between cancer and healthy cells. This situation results in side-effects during antitumoral treatments. For this reason, recent studies are on nanocarriers with ligands that bind to the specific cells or tissues and increase tumoral uptake ability. Some of these ligands are nucleic acids, antibodies, peptides and some other molecules. These site-specific drug delivery systems serve targeted delivery with controlled and sustained release (Cheng et al., 2017).

Nanostructures used in drug delivery enables binding to cancer specific receptors by targeting ligand. Some of the ligand receptors are lectin receptors, complement receptors, interleukin receptors, and lipoprotein receptors and dopamine receptors. Dopamine is

monoamine catecholamine neurotransmitter and it is very important for central nervous system of brain (Masoudipour et al., 2017). Additionally, polydopamine (PDA) creates adhesive layer on materials and it enables a surface for secondary reactions. Thus, ligand molecules having functional groups such as thiol or amine can be placed on PDA structures (Cheng et al., 2017). Dopamine receptor containing nanostructures can be operated for targeted drug delivery.

Folate receptors are glycophosphatidylinositol linked receptor and they are considered as folate binding glycoprotein membranes. They present in human tumor cells and that is why it is applied in targeted drug delivery studies (Barar et al., 2015). On the other hand, folic acid (FA) is water soluble vitamin B and it is nonimmunogenic and stable. It can bind to folate receptors selectively. Hence, FA can be incorporated to nanocarriers for controlled and targeted drug delivery (Cheng et al., 2017).

The scope of this study is to synthesize pH responsive coaxial nanotubes with folate receptor targeting for cancer treatment applications. Coaxial nanotubes are fabricated with the outer side of polydopamine-folic acid and inner side of poly(methacrylic acid-*co*-ethylene glycol dimethacrylate) p(MAA-*co*-EGDMA). iCVD technique involving free radical polymerization is used for pH responsive, non-soluble p(MAA-*co*-EGDMA) nanotubes fabrication. Conformal deposition is achieved by AAO template. Due to vapor phase synthesis, disadvantages of solution-based fabrication methods as solvent toxicity can be prevented in iCVD fabrication. Structures and compositions of nanotubes are characterized by scanning electron microscopy and Fourier transform infrared spectroscopy. Thickness measurements and swelling behavior are investigated by ellipsometry. Drug loading and release mechanisms are studied using model drug molecule.

4.2. Materials and Methods

Preparation of Polydopamine-Folic Acid Nanotubes

Polydopamine-Folic acid nanotubes were prepared by adding 12 g Tris, 0.37 g dopamine and 0.12 g folic acid into a beaker. To adjust pH at 8.7, 50 ml DI water and 52 ml 1 M sodium hydroxide (NaOH) were added to the solution. After pH adjustment, the solution became

homogeneous. The solution is then transferred to the a prolate beaker. In the solution, AAO templates were put vertically by using a stage. AAO templates were waited in the dopamine-folic acid solution overnight by stirring it at 100 rpm. After 24h, solution was drawn by pipette and PDA-FA coated AAO templates were put into DI water for 5 minutes to get rid of residual dopamine and FA.

Deposition of Polydopamine-Folic Acid Nanotubes

Coaxial p(MAA-*co*-EGDMA)/PDA-FA nanotubes were synthesized on PDA-FA coated AAO templates by iCVD involving free radical chain-growth polymerization of a conjugated polymer. Filament and substrate temperatures were 240°C and 25°C, respectively. Chamber pressure was adjusted to 200 mTorr. Flow rates were determined 3.16 sccm for MAA at 65°C and 0.32 sccm for EGDMA at 95°C. Initiator (TBPO) and nitrogen were given 1.06 sccm and 1.29 sccm. Deposition thickness was 200 nm.

Loading and Release Studies of Coaxial Nanotubes

Samples were immersed in 1M hydrochloric acid (HCl) solution and rinsed after deposition to etch AAO templates. Coaxial polymeric nanotubes were waited in 1 g/ml RB solution at pH 9 for loading. After 24 hours, nanotubes were put into DI water at pH4 and release from nanotubes were achieved at pH 4. At 0h and and 24h of loading, 100µL of solution was taken. By subtracting the concentration at 24h from the one at 0h, loading concentration was calculated.

UV-Vis measurement was performed via NanoDrop UV-Vis spectrophotometer (Thermo Scientific NanoDrop 2000c). For each measurement, 2µL of solution taken at specified time intervals were used. Release concentrations were calculated via calibration curve. By using Korsmeyer-Peppas equation, release kinetics were modelled.

4.3. Results and Discussion

SEM images confirmed open cylindrical structures of coaxial nanotubes. Figure 13 shows p(MAA-*co*-EGDMA)/PDA-FA nanotubes before etching. The rigidity represents the presence of AAO templates. Figure 14 reveals the etched nanotubes.

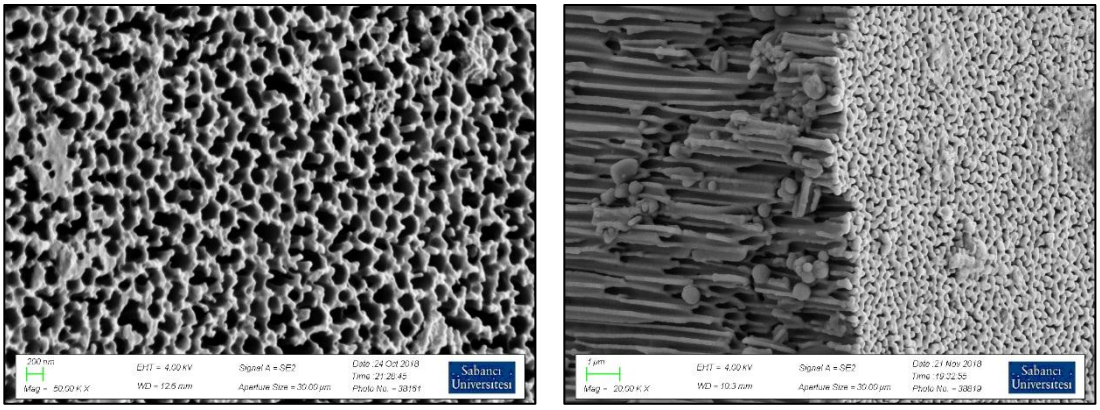

Figure 13. Top and Cross-sectional images of non-etched p(MAA-*co*-EGDMA)/PDA-FA nanotubes.

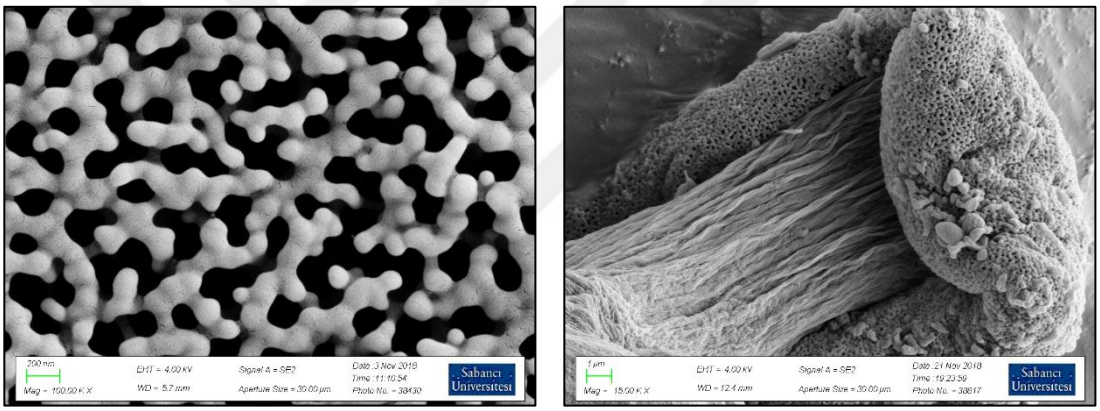

Figure 14. Top and Cross-sectional images of etched p(MAA-*co*-EGDMA)/PDA-FA nanotubes.

FTIR spectra of p(MAA-*co*-EGDMA) thin film is shown in Fig 15. At wavenumber 1636.98 cm^{-1}, C=O stretching of MAA, and at 1729.68 cm^{-1}, C=O stretching of EGDMA are observed. At 2959.93 cm^{-1}, C-H stretching, and at 3508.6 cm^{-1}, O-H stretching present FTIR spectra confirms the deposition of PDA-FA nanotubes.

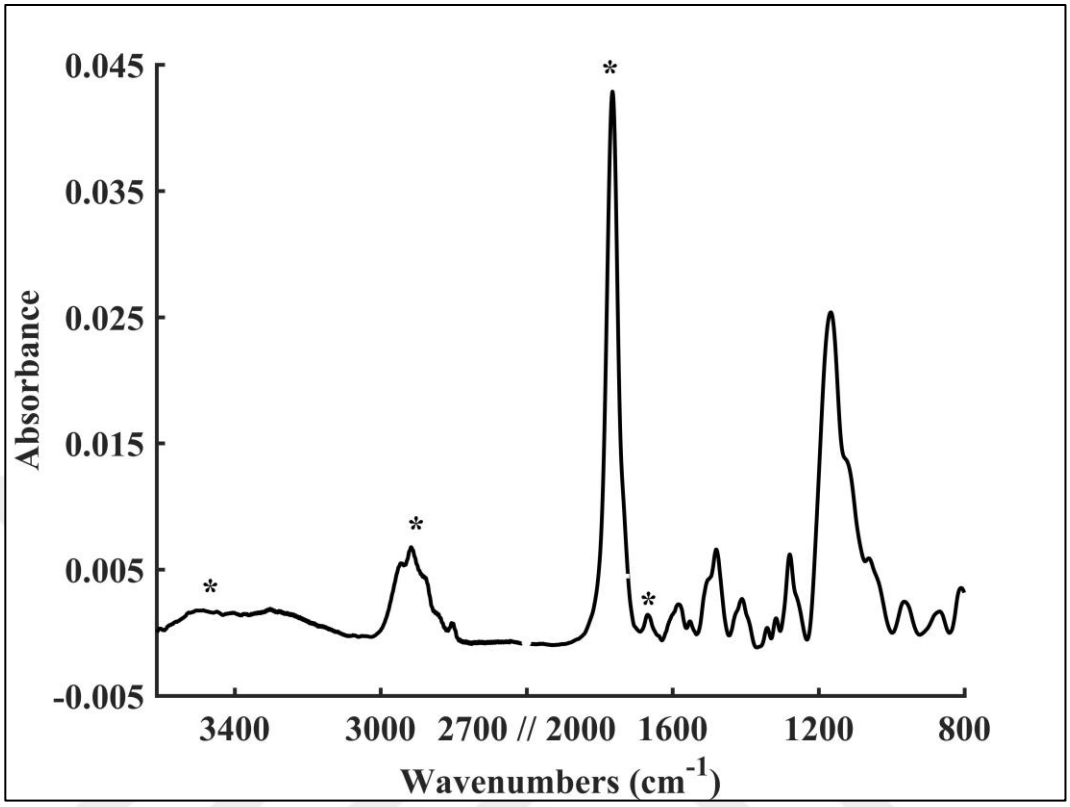

Figure 15. FTIR spectra of p(MAA-*co*-EGDMA) thin films.

Swelling behaviour of p(MAA-co-EGDMA) thin films were investigated by liquid cell ellipsometer. At pH 4, thickness of thin film increases from 156.55±0.423 nm to 169.79±0.423 nm. At pH 9, thickness change is from 200.89±3.094 nm to 286.25±3.094 nm. The swelling ratio is 8.5% for pH 4 and 42.5% for pH 9. These results concludes that p(MAA-co-EGDMA) is pH responsive and it is suitable for controlled drug delivery. According to these ratios, RB loading is achieved at pH 9 where the swelling is higher and RB release is performed at pH 4 where collapsing occurs (Fig 16).

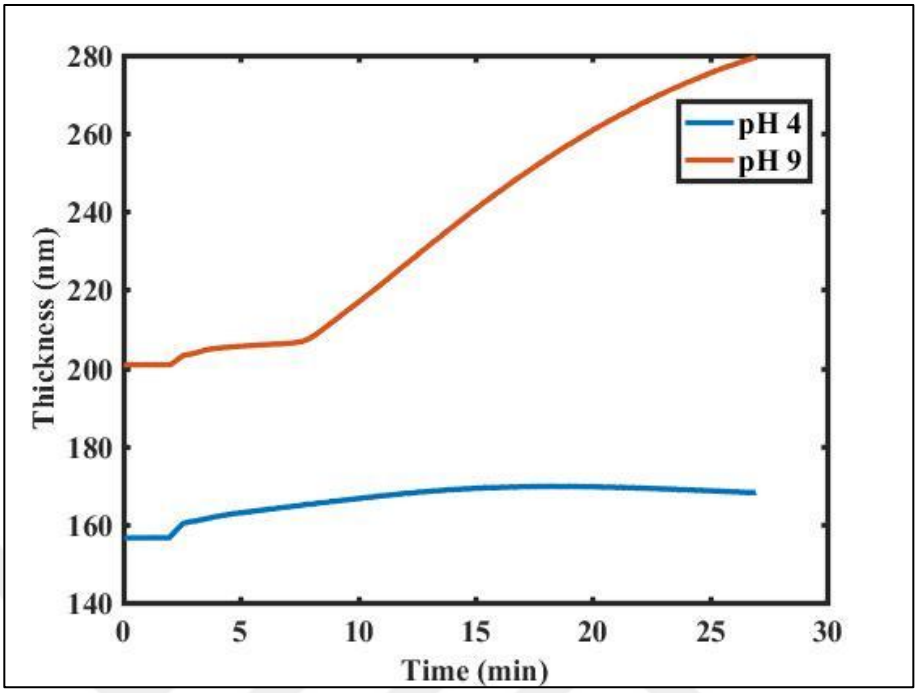

Figure 16. Swelling behaviour of p(MAA-*co*-EGDMA) thin films.

For release studies, concentration of RB at specified time intervals were measured and then the percentages were calculated by using the loading concentration which is 0.118 mg/ml. Maximum release was achieved at 48th hour with the percentage of 44%. According to Korsmeyer-Peppas kinetic model, data is fitted to the equation. R^2 was found 0.93. The Peppas parameters were given in Table 3. n is found 0.29 that demonstrates the Fickian diffusion model. Data fitted release profile was shown in Figure 17.

Table 3. Korsmeyer-Peppas parameters of release profiles from p(MAA-*co*-EGDMA)/PDA-FA nanotubes.

	Korsmeyer-Peppas Parameters		
	R^2	n	a
pH 4	0.93	0.29	0.1534

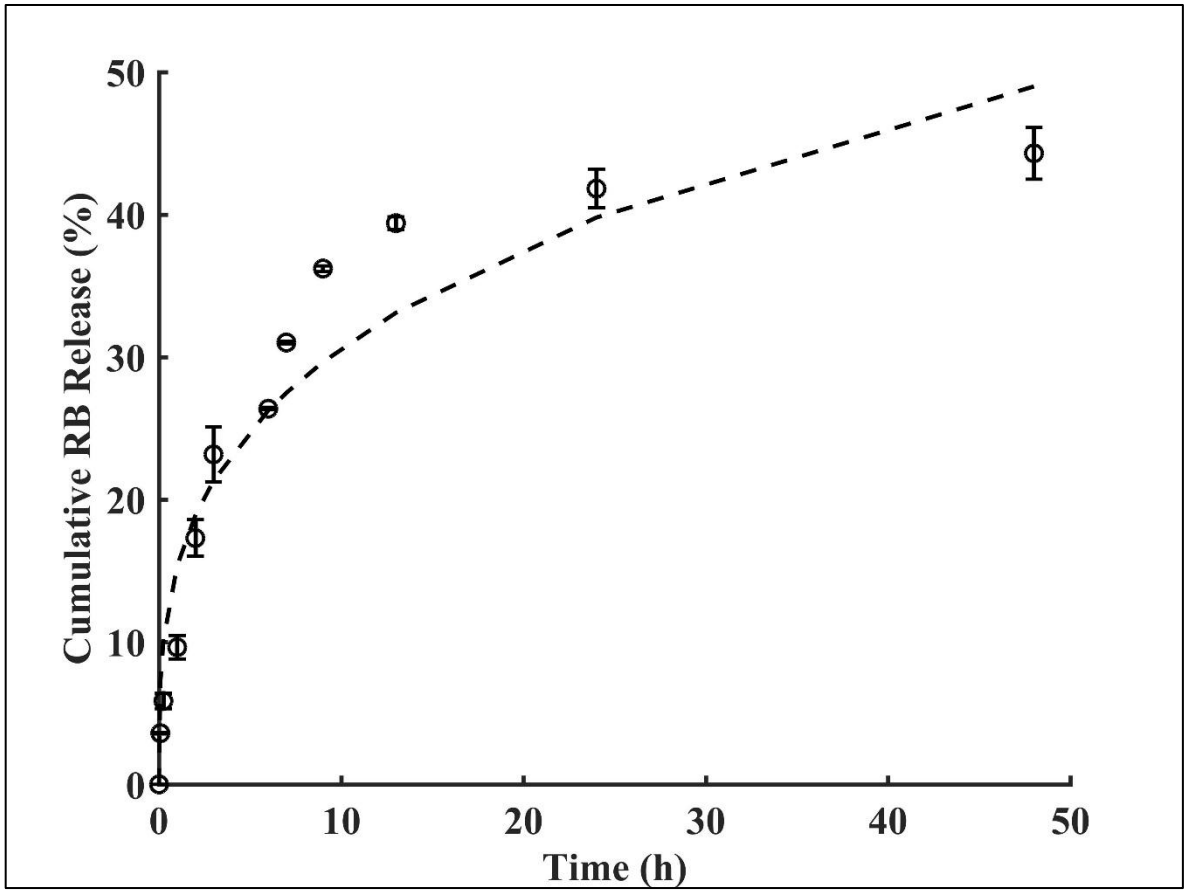

Figure 17. Release profiles from p(MAA-*co*-EGDMA)/PDA-FA nanotubes.

4.4. Conclusion

Biocompatible and biodegradable PDA-FA nanotubes having high affinity to bind folate receptors were synthesized. P(MAA-co-EGDMA) deposition resulting coaxial nanotubes provides pH response for controlled drug delivery. Enhanced surface are/volume ratio is expected to provide longer residence time. As forthcoming research, binding of these nanocarriers to folate receptors will ve investigated in vitro.

CHAPTER 5

FABRICATION OF DUAL RESPONSIVE NANOTUBES FOR CONTROLLED RELEASE

5.1. Introduction

Targeting and having single stimuli responsive structures were investigated so far. By using coated fibers and coaxial nanotubes with targeting agents, release kinetics were adjusted. To improve control over release, more complex structures were required. Accordingly, nanotubes having more than one stimulus response were studied.

Progressive studies in controlled drug delivery includes dual responsive DDS. These systems have smart materials with more than one stimulus response simultaneously and they are advantageous in biomedical applications. Release kinetics can be adjusted according to the optimum stimuli parameters and better control can be achieved (Cabane et al., 2012). These multiple responsive nanocarriers depends on the polymer structures. For example, random copolymers are synthesized to have pH- and temperature response whereas copolymers that are self-assemble can form micelles with different environmental conditions (Schmaljohann, 2006).

In this study, poly(n-[3-(dimethylamino)propyl]methacrylamide-*co*-ethylene glycol dimethacrylate) p(DMAPMA-*co*-EGDMA) nanotubes were synthesized by iCVD using AAO templates. This polymer is both thermo- and CO_2 responsive. At different temperature conditions and both in N_2 and CO_2 ambient, RB release was investigated.

5.2. Materials and Methods

p(DMAPMA-*co*-EGDMA) nanotubes were fabricated by using iCVD. Filament and substrate temperatures were 240°C and 25°C, respectively. DMAPMA at 130°C were given to the system with 0.1935 sccm and EGDMA at 95°C was applied with 0.1238 sccm. Reaction pressure was kept at 200 mTorr. N_2 and TBPO were fed at 0.9418 sccm and 0.9596 sccm. Thickness of the deposition was 300 nm.

AAO was etched by waiting coated AAO templates in 1 M HCl overnight and then by rinsing. Samples were waited in RB solution for 46 hours and then rinsed again to remove residual RB on nanotubes.

4 set of samples were put in 3 necked round bottom flasks with 10 ml DI water. Two of them were at room temperature in N_2 and CO_2 environment, separately. Other two were at 50°C and in N_2 and CO_2. Release data were obtained by using Nanodrop UV-Vis spectroscopy.

5.3. Results and Discussion

SEM images in Figure 18 confirm p(DMAPMA-*co*-EGDMA) nanotubes formation. Etched samples show the open top of the cylindrical structures.

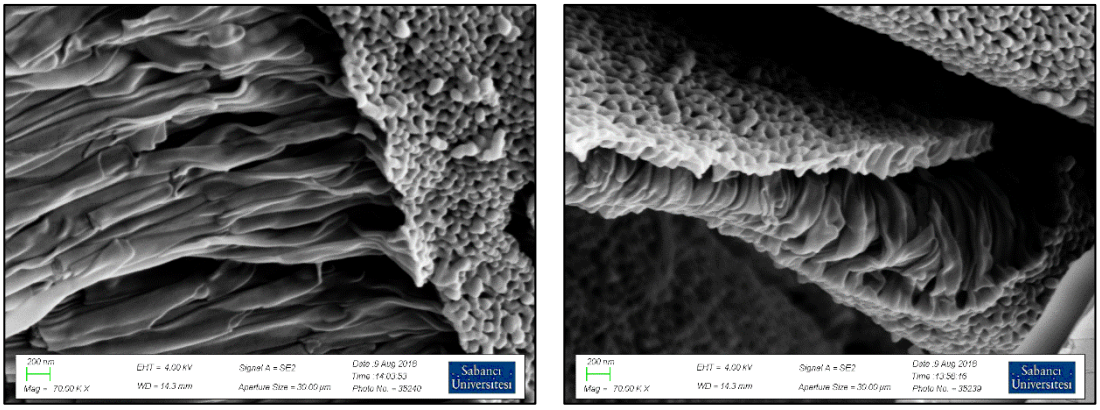

Figure 18. SEM Images of etched p(DMAPMA-*co*-EGDMA) nanotubes.

FTIR spectra of p(DMAPMA-*co*-EGDMA) thin film was shown in Figure 19. Peaks at 3363 cm^{-1}, 1653 cm^{-1}, and 1520 cm^{-1} represents the N-H stretching, amide I and amide II, respectively. At 1733 cm^{-1}, C=O stretching of EGDMA is shown (Mishra and Ray, 2010).

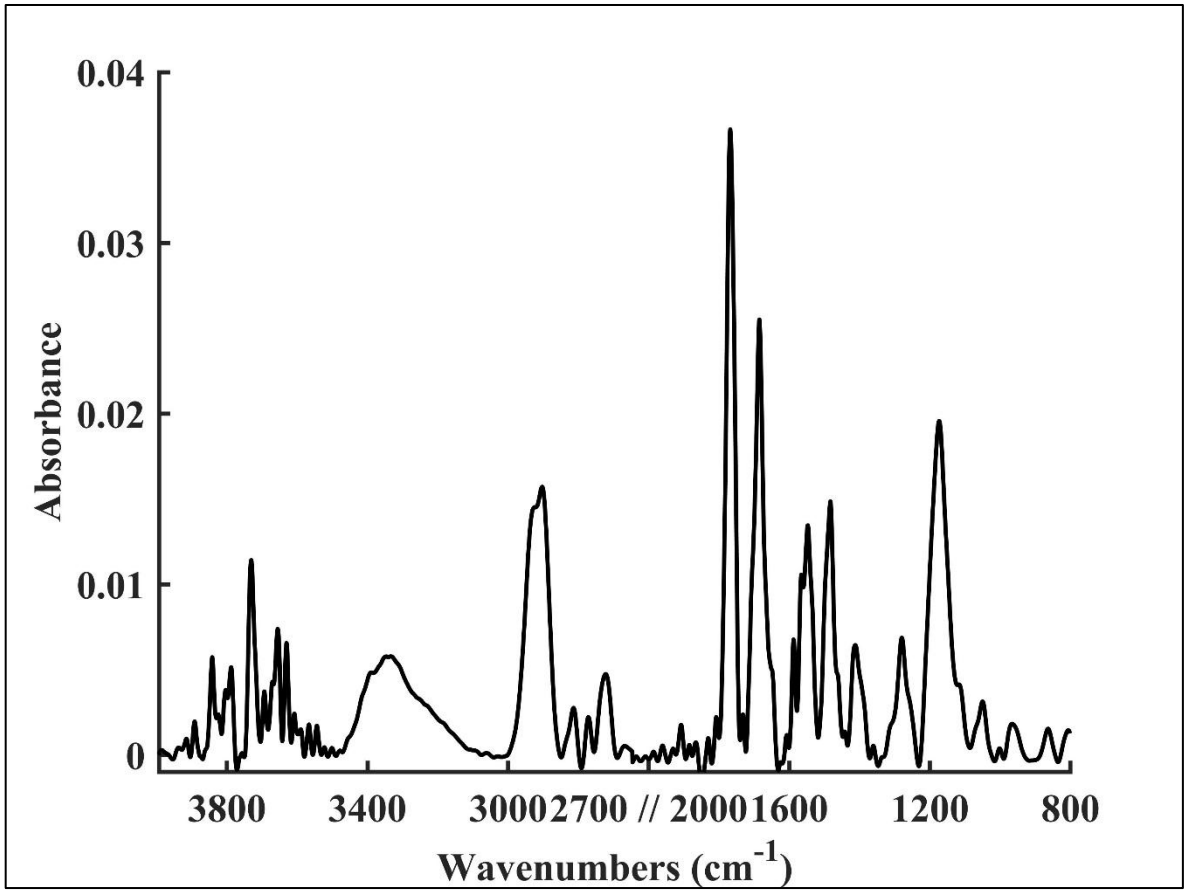

Figure 19. FTIR spectra of p(DMAPMA-*co*-EGDMA) thin films.

Release behavior of p(DMAPMA-*co*-EGDMA) nanotubes were investigated and shown in Figure 20. RB release was performed at room temperature, at 50°C, in the N_2 and CO_2 conditions for 24 hours. The maximum release was obtained at 50°C in N_2 with 94%. According to profiles, p(DMAPMA-*co*-EGDMA) nanotubes showed both temperature and CO_2 response. The drug release is sustained and controlled with temperature increase and CO_2 application. Thus, thermo and CO_2 responsivity can be tuned with N_2 and CO_2 application.

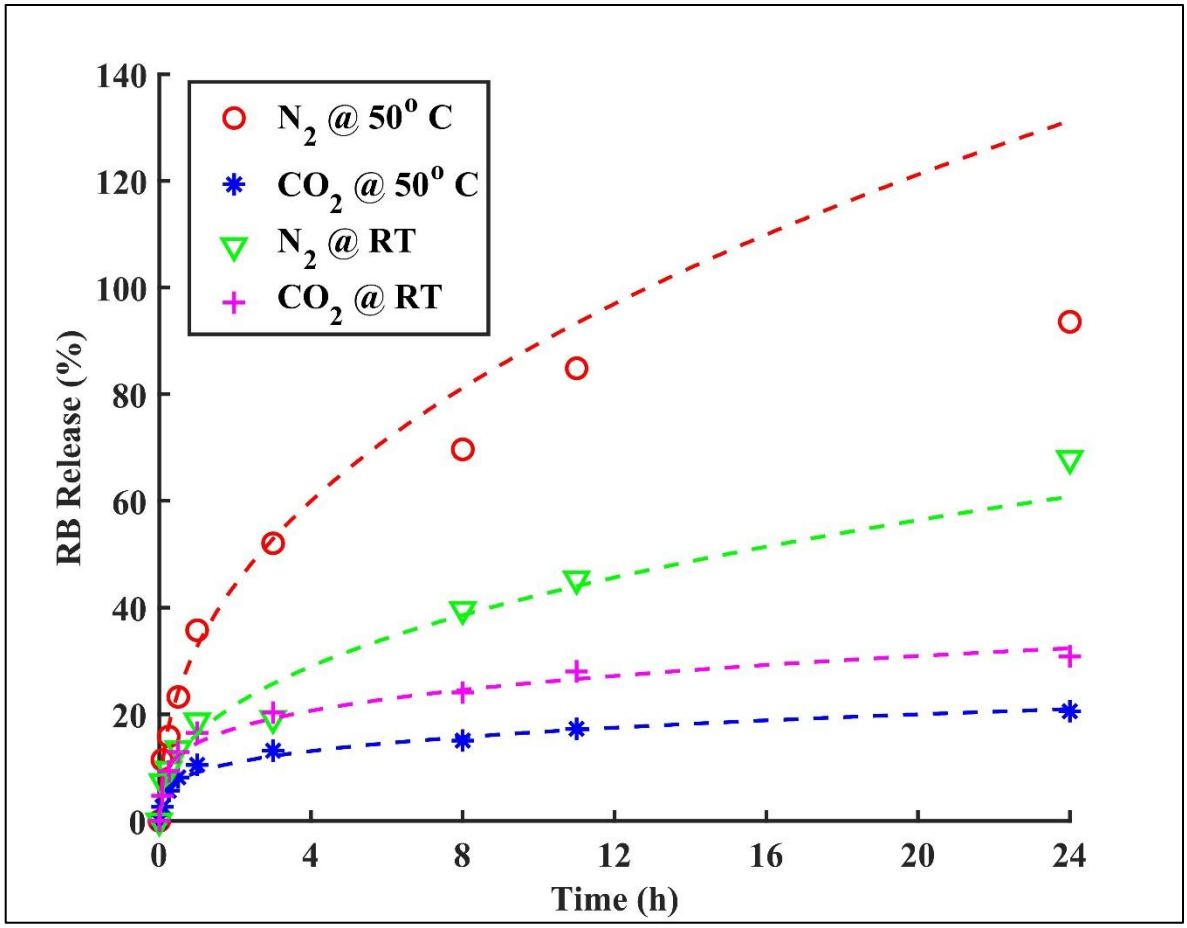

Figure 20. Release profiles from p(DMAPMA-*co*-EGDMA) nanotubes at different gas ambient and temperatures.

Release kinetics were investigated according to Korsmeyer-Peppas equation. Parameters were given in Table 4. According to n values, release kinetics were found to obey Fickian diffusion. Release from CO_2 applied samples were slower than the N_2 ambient.

Table 4. Korsmeyer-Peppas parameters of release profiles from p(DMAPMA-*co*-EGDMA) nanotubes.

	Room temp			**50° C**		
	R^2	n	a	R^2	n	a
N_2	0.97	0.42	0.1633	0.99	0.43	0.3274
CO_2	0.98	0.25	0.1459	0.98	0.26	0.9117

5.4. Conclusion

Dual responsive polymeric nanostructures gained attention in recent years with respect to tuning controlled drug delivery. p(DMAPMA-*co*-EGDMA) nanotubes were fabricated for temperature and CO_2 response and delivery of RB. Release kinetics showed that all the conditions results in Fickian diffusion model. Additionally, CO_2 and temperature application revealed sustained release within 24 hours.

CONCLUSION

This work focuses on the one-dimensional stimuli responsive nanofiber and nanotube synthesis for drug delivery applications. Enhanced surface area-volume ratio enables increased efficiency on controlling release mechanism. First part involves combined methods of electrospinning and iCVD. PVA-RB blend nanofibers were coated with pH-responsive, insoluble p(4VP-*co*-EGDMA) polymer conformally to form coaxial nanofiber mat. At pH 4, pH 6.5 and pH 9, release mechanisms were investigated. Due to swelling and collapsing behavior, at lower pH values, decreased drug dosage and sustained release were obtained. In the second chapter, coaxial p(MAA-*co*-EGDMA)/PDA-FA nanotubes were synthesized by combined solution-based and iCVD methods. AAO templated nanotube synthesis resulted in RB loading at higher pH values and release at lower pH values due to pH response of p(MAA-*co*-EGDMA) inner layer. Additionally, polydopamine and folic acid act as targeting agents to tumor cells. In the final chapter, dual temperature and CO_2 responsive p(DMAPMA-*co*-EGDMA) nanotubes were formed via iCVD technique. These tubes resulted in sustained release when CO_2 and temperature are both applied simultaneously. As a result, polymeric nanotubes and nanofibers are promising for drug delivery applications with their targeted and responsive features.

BIBLIOGRAPHY

Abidian, M. R., Kim, D. H., & Martin, D. C. (2006). Conducting-polymer nanotubes for controlled drug release. *Advanced materials*, *18*(4), 405-409.

Al-Enizi, A., Zagho, M., & Elzatahry, A. (2018). Polymer-based electrospun nanofibers for biomedical applications. *Nanomaterials*, *8*(4), 259.

Aljehani, A. K., Hussaini, M. A., Hussain, M. A., Alothmany, N. S., & Aldhaheri, R. W. (2014, February). Effect of electrospinning parameters on nanofiber diameter made of poly (vinyl alcohol) as determined by Atomic Force Microscopy. In *2nd Middle East Conference on Biomedical Engineering* (pp. 379-381). IEEE.

Alf, M. E., Asatekin, A., Barr, M. C., Baxamusa, S. H., Chelawat, H., Ozaydin-Ince, G., ... & Vaddiraju, S. (2010). Chemical vapor deposition of conformal, functional, and responsive polymer films. *Advanced Materials*, *22*(18), 1993-2027.

Ali, A., & Ahmed, S. (2018). A review on chitosan and its nanocomposites in drug delivery. *International journal of biological macromolecules*, *109*, 273-286.

Allen, T. M., & Cullis, P. R. (2004). Drug delivery systems: entering the mainstream. *Science*, *303*(5665), 1818-1822.

Armagan, E., & Ince, G. O. (2015). Coaxial nanotubes of stimuli responsive polymers with tunable release kinetics. *Soft matter*, *11*(41), 8069-8075.

Barar, J., Kafil, V., Majd, M. H., Barzegari, A., Khani, S., Johari-Ahar, M., ... & Omidi, Y. (2015). Multifunctional mitoxantrone-conjugated magnetic nanosystem for targeted therapy of folate receptor-overexpressing malignant cells. *Journal of nanobiotechnology*, *13*(1), 26.

Baxamusa, S. H., Im, S. G., & Gleason, K. K. (2009). Initiated and oxidative chemical vapor deposition: a scalable method for conformal and functional polymer films on real substrates. *Physical Chemistry Chemical Physics*, *11*(26), 5227-5240.

Bayari, S., & Yurdakul, Ş. (2000). Fourier transform infrared and Raman spectra of 4-vinylpyridine and its transition metal (II) tetracyanonickelate complexes. *Spectroscopy Letters*, *33*(4), 475-483.

Bazhban, M., Nouri, M., & Mokhtari, J. (2013). Electrospinning of cyclodextrin functionalized chitosan/PVA nanofibers as a drug delivery system. *Chinese Journal of Polymer Science*, *31*(10), 1343-1351.

Brown III, C. L., & Crawford, N. (2002). *U.S. Patent No. 6,424,862*. Washington, DC: U.S. Patent and Trademark Office.

Cabane, E., Zhang, X., Langowska, K., Palivan, C. G., & Meier, W. (2012). Stimuli-responsive polymers and their applications in nanomedicine. *Biointerphases*, *7*(1), 9.

Chakraborty, S., Liao, I. C., Adler, A., & Leong, K. W. (2009). Electrohydrodynamics: a facile technique to fabricate drug delivery systems. *Advanced drug delivery reviews*, *61*(12), 1043-1054.

Chen, G. (2012). Nanotube-Based Controlled Drug Delivery. *Pharmaceut Anal Acta*, *3*(9), 2153-2435.

Chen, G., Chen, R., Zou, C., Yang, D., & Chen, Z. S. (2014). Fragmented polymer nanotubes from sonication-induced scission with a thermo-responsive gating system for anti-cancer drug delivery. *Journal of Materials Chemistry B*, *2*(10), 1327-1334.

Chen, S., Li, R., Li, X., & Xie, J. (2018). Electrospinning: An enabling nanotechnology platform for drug delivery and regenerative medicine. *Advanced drug delivery reviews*, *132*, 188-213.

Cheng, W., Nie, J., Xu, L., Liang, C., Peng, Y., Liu, G., ... & Zeng, X. (2017). pH-sensitive delivery vehicle based on folic acid-conjugated polydopamine-modified mesoporous silica nanoparticles for targeted cancer therapy. *ACS applied materials & interfaces*, *9*(22), 18462-18473.

Chunder, A., Sarkar, S., Yu, Y., & Zhai, L. (2007). Fabrication of ultrathin polyelectrolyte fibers and their controlled release properties. *Colloids and Surfaces B: Biointerfaces*, *58*(2), 172-179.

Coelho, J. F., Ferreira, P. C., Alves, P., Cordeiro, R., Fonseca, A. C., Góis, J. R., & Gil, M. H. (2010). Drug delivery systems: Advanced technologies potentially applicable in personalized treatments. *EPMA journal*, *1*(1), 164-209.

Costa, P., & Lobo, J. M. S. (2001). Modeling and comparison of dissolution profiles. *European journal of pharmaceutical sciences*, *13*(2), 123-133.

Crespy, D., & Rossi, R. M. (2007). Temperature-responsive polymers with LCST in the physiological range and their applications in textiles. *Polymer International*, *56*(12), 1461-1468.

Croisier, F., Atanasova, G., Poumay, Y., & Jérôme, C. (2014). Polysaccharide-Coated PCL Nanofibers for Wound Dressing Applications. *Advanced healthcare materials*, *3*(12), 2032-2039.

Dabrzalska, M., Benseny-Cases, N., Barnadas-Rodríguez, R., Mignani, S., Zablocka, M., Majoral, J. P., ... & Cladera, J. (2016). Fourier transform infrared spectroscopy (FTIR) characterization of the interaction of anti-cancer photosensitizers with dendrimers. *Analytical and bioanalytical chemistry*, *408*(2), 535-544.

Dai, S., Ravi, P., & Tam, K. C. (2008). pH-Responsive polymers: synthesis, properties and applications. *Soft Matter*, *4*(3), 435-449.

Demirci, S., Celebioglu, A., Aytac, Z., & Uyar, T. (2014). pH-responsive nanofibers with controlled drug release properties. *Polymer Chemistry*, *5*(6), 2050-2056.

Fu, Y., & Kao, W. J. (2010). Drug release kinetics and transport mechanisms of non-degradable and degradable polymeric delivery systems. *Expert opinion on drug delivery*, *7*(4), 429-444.

Gao, Y., Wei, M., Li, X., Xu, W., Ahiabu, A., Perdiz, J., ... & Serpe, M. J. (2017). Stimuli-responsive polymers: Fundamental considerations and applications. *Macromolecular Research*, *25*(6), 513-527.

Garg, T., Malik, B., Rath, G., & Goyal, A. K. (2014). Development and characterization of nano-fiber patch for the treatment of glaucoma. *European Journal of Pharmaceutical Sciences*, *53*, 10-16.

Gencturk, A., Kahraman, E., Güngör, S., Özhan, G., Özsoy, Y., & Sarac, A. S. (2017). Polyurethane/hydroxypropyl cellulose electrospun nanofiber mats as potential transdermal drug delivery system: characterization studies and in vitro assays. *Artificial cells, nanomedicine, and biotechnology*, *45*(3), 655-664.

Goldberg, M., Langer, R., & Jia, X. (2007). Nanostructured materials for applications in drug delivery and tissue engineering. *Journal of Biomaterials Science, Polymer Edition*, *18*(3), 241-268.

González, E., & Frey, M. W. (2017). Synthesis, characterization and electrospinning of poly (vinyl caprolactam-co-hydroxymethyl acrylamide) to create stimuli-responsive nanofibers. *Polymer*, *108*, 154-162.

He, C. L., Huang, Z. M., Han, X. J., Liu, L., Zhang, H. S., & Chen, L. S. (2006). Coaxial electrospun poly (L-lactic acid) ultrafine fibers for sustained drug delivery. *Journal of Macromolecular Science, Part B*, *45*(4), 515-524.

Hrib, J., Sirc, J., Hobzova, R., Hampejsova, Z., Bosakova, Z., Munzarova, M., & Michalek, J. (2015). Nanofibers for drug delivery–incorporation and release of model molecules, influence of molecular weight and polymer structure. *Beilstein journal of nanotechnology*, *6*(1), 1939-1945.

Huang, R. Y. M., & Rhim, J. W. (1993). Modification of poly (vinyl alcohol) using maleic acid and its application to the separation of acetic acid-water mixtures by the pervaporation technique. *Polymer international*, *30*(1), 129-135.

Ince, G. O., Demirel, G., Gleason, K. K., & Demirel, M. C. (2010). Highly swellable free-standing hydrogel nanotube forests. *Soft Matter*, *6*(8), 1635-1639.

Jalvandi, J., White, M., Gao, Y., Truong, Y. B., Padhye, R., & Kyratzis, I. L. (2017). Polyvinyl alcohol composite nanofibres containing conjugated levofloxacin-chitosan for controlled drug release. *Materials Science and Engineering: C*, *73*, 440-446.

Jannesari, M., Varshosaz, J., Morshed, M., & Zamani, M. (2011). Composite poly (vinyl alcohol)/poly (vinyl acetate) electrospun nanofibrous mats as a novel wound dressing matrix for controlled release of drugs. *International journal of nanomedicine*, *6*, 993.

Kenawy, E. R., Abdel-Hay, F. I., El-Newehy, M. H., & Wnek, G. E. (2007). Controlled release of ketoprofen from electrospun poly (vinyl alcohol) nanofibers. *Materials Science and Engineering: A*, *459*(1-2), 390-396.

Kenawy, E. R., Abdel-Hay, F. I., El-Newehy, M. H., & Wnek, G. E. (2009). Processing of polymer nanofibers through electrospinning as drug delivery systems. In *Nanomaterials: Risks and Benefits* (pp. 247-263). Springer, Dordrecht.

Kenawy, E. R., Bowlin, G. L., Mansfield, K., Layman, J., Simpson, D. G., Sanders, E. H., & Wnek, G. E. (2002). Release of tetracycline hydrochloride from electrospun poly (ethylene-co-vinylacetate), poly (lactic acid), and a blend. *Journal of controlled release*, *81*(1-2), 57-64.

Khajavi, R., & Abbasipour, M. (2012). Electrospinning as a versatile method for fabricating coreshell, hollow and porous nanofibers. *Scientia Iranica*, *19*(6), 2029-2034.

Kim, Y. J., Ebara, M., & Aoyagi, T. (2013). A smart hyperthermia nanofiber with switchable drug release for inducing cancer apoptosis. *Advanced Functional Materials*, *23*(46), 5753-5761.

Kocak, G., Tuncer, C., & Bütün, V. (2017). pH-Responsive polymers. *Polymer Chemistry*, *8*(1), 144-176.

Koevary, S. B. (2012). Selective toxicity of rose bengal to ovarian cancer cells in vitro. *International journal of physiology, pathophysiology and pharmacology*, *4*(2), 99.

Korsmeyer, R. W., Gurny, R., Doelker, E., Buri, P., & Peppas, N. A. (1983). Mechanisms of solute release from porous hydrophilic polymers. *International journal of pharmaceutics*, *15*(1), 25-35.

Kost, J., & Langer, R. (2012). Responsive polymeric delivery systems. *Advanced drug delivery reviews*, *64*, 327-341.

Langer, R. (1998). Drug delivery and targeting. *NATURE-LONDON-*, 5-10.

LaPorte, S., Haller, M., Hooper, W., Lent, M., Riff, K., Heruth, K., & Olsen, J. (2005). *U.S. Patent Application No. 10/137,516*.

Lau, K. K., & Gleason, K. K. (2006). Initiated chemical vapor deposition (iCVD) of poly (alkyl acrylates): an experimental study. *Macromolecules*, *39*(10), 3688-3694.

Lau, K. K., & Gleason, K. K. (2007). All-dry synthesis and coating of methacrylic acid copolymers for controlled release. *Macromolecular bioscience*, *7*(4), 429-434.

Li, D., He, Q., Yang, Y., Möhwald, H., & Li, J. (2008). Two-stage pH response of poly (4-vinylpyridine) grafted gold nanoparticles. *Macromolecules*, *41*(19), 7254-7256.

Li, W., Xu, R., Zheng, L., Du, J., Zhu, Y., Huang, R., & Deng, H. (2012). LBL structured chitosan-layered silicate intercalated composites based fibrous mats for protein delivery. *Carbohydrate polymers*, *90*(4), 1656-1663.

Li, X., Kanjwal, M. A., Lin, L., & Chronakis, I. S. (2013). Electrospun polyvinyl-alcohol nanofibers as oral fast-dissolving delivery system of caffeine and riboflavin. *Colloids and Surfaces B: Biointerfaces*, *103*, 182-188.

Liu, H., Lin, S., Feng, Y., & Theato, P. (2017). CO 2-responsive polymer materials. *Polymer Chemistry*, *8*(1), 12-23.

Long, Y. Z., Li, M. M., Gu, C., Wan, M., Duvail, J. L., Liu, Z., & Fan, Z. (2011). Recent advances in synthesis, physical properties and applications of conducting polymer nanotubes and nanofibers. *Progress in Polymer Science*, *36*(10), 1415-1442.

Mansur, H. S., Sadahira, C. M., Souza, A. N., & Mansur, A. A. (2008). FTIR spectroscopy characterization of poly (vinyl alcohol) hydrogel with different hydrolysis degree and chemically crosslinked with glutaraldehyde. *Materials Science and Engineering: C*, *28*(4), 539-548.

Masoudipour, E., Kashanian, S., & Maleki, N. (2017). A targeted drug delivery system based on dopamine functionalized nano graphene oxide. *Chemical Physics Letters*, *668*, 56-63.

Meng, Z. X., Xu, X. X., Zheng, W., Zhou, H. M., Li, L., Zheng, Y. F., & Lou, X. (2011). Preparation and characterization of electrospun PLGA/gelatin nanofibers as a potential drug delivery system. *Colloids and Surfaces B: Biointerfaces*, *84*(1), 97-102.

Mickova, A., Buzgo, M., Benada, O., Rampichova, M., Fisar, Z., Filova, E., ... & Amler, E. (2012). Core/shell nanofibers with embedded liposomes as a drug delivery system. *Biomacromolecules*, *13*(4), 952-962.

Mishra, R. K., & Ray, A. R. (2011). Synthesis and characterization of poly {N-[3-(dimethylamino) propyl] methacrylamide-co-itaconic acid} hydrogels for drug delivery. *Journal of Applied Polymer Science*, *119*(6), 3199-3206.

Mu, C., & Wu, Q. (2017). Electrospun Poly (ε-caprolactone) Composite Nanofibers with Controlled Release of Cis-Diamminediiodoplatinum for a Higher Anticancer Activity. *Nanoscale research letters*, *12*(1), 318.

Mura, S., Nicolas, J., & Couvreur, P. (2013). Stimuli-responsive nanocarriers for drug delivery. *Nature materials*, *12*(11), 991.

Nelson, K. D., Romero-Sanchez, A. A., Smith, G. M., Alikacem, N., Radulescu, D., Waggoner, P., & Hu, Z. (2003). *U.S. Patent No. 6,596,296*. Washington, DC: U.S. Patent and Trademark Office.

Newland, B., Taplan, C., Pette, D., Friedrichs, J., Steinhart, M., Wang, W., ... & Werner, C. (2018). Soft and flexible poly (ethylene glycol) nanotubes for local drug delivery. *Nanoscale*, *10*(18), 8413-8421.

Nguyen, T. T. T., Ghosh, C., Hwang, S. G., Chanunpanich, N., & Park, J. S. (2012). Porous core/sheath composite nanofibers fabricated by coaxial electrospinning as a potential mat for drug release system. *International journal of pharmaceutics*, *439*(1-2), 296-306.

Ohkawa, K., Cha, D., Kim, H., Nishida, A., & Yamamoto, H. (2004). Electrospinning of chitosan. *Macromolecular Rapid Communications*, *25*(18), 1600-1605.

Oliveira, M. F., Suarez, D., Rocha, J. C. B., de Carvalho Teixeira, A. V. N., Cortés, M. E., De Sousa, F. B., & Sinisterra, R. D. (2015). Electrospun nanofibers of polyCD/PMAA polymers and their potential application as drug delivery system. *Materials Science and Engineering: C*, *54*, 252-261.

Ozaydin-Ince, G., & Gleason, K. K. (2010). Tunable conformality of polymer coatings on high aspect ratio features. *Chemical Vapor Deposition*, *16*(1-3), 100-105.

Ozaydin-Ince, G., Coclite, A. M., & Gleason, K. K. (2011). CVD of polymeric thin films: applications in sensors, biotechnology, microelectronics/organic electronics, microfluidics, MEMS, composites and membranes. *Reports on Progress in Physics*, *75*(1), 016501.

Ozaydin-Ince, G., Gleason, K. K., & Demirel, M. C. (2011). A stimuli-responsive coaxial nanofilm for burst release. *Soft Matter*, *7*(2), 638-643.

Parhi, P., Mohanty, C., & Sahoo, S. K. (2012). Nanotechnology-based combinational drug delivery: an emerging approach for cancer therapy. *Drug discovery today*, *17*(17-18), 1044-1052.

Pillay, V., Dott, C., Choonara, Y. E., Tyagi, C., Tomar, L., Kumar, P., ... & Ndesendo, V. M. (2013). A review of the effect of processing variables on the fabrication of electrospun nanofibers for drug delivery applications. *Journal of Nanomaterials*

Piras, A. M., Chiellini, F., Chiellini, E., Nikkola, L., & Ashammakhi, N. (2008). New multicomponent bioerodible electrospun nanofibers for dual-controlled drug release. *Journal of Bioactive and Compatible Polymers*, *23*(5), 423-443.

Purvya, M. C., & Meena, M. S. (2011). A review on role of prakriti in aging. *Ayu*, *32*(1), 20.

Qin, J., Kunda, N., Qiao, G., Calata, J. F., Pardiwala, K., Prabhakar, B. S., & Maker, A. V. (2017). Colon cancer cell treatment with rose bengal generates a protective immune response via immunogenic cell death. *Cell death & disease*, *8*(2), e2584.

Ramteke, K. H., Dighe, P. A., Kharat, A. R., & Patil, S. V. (2014). Mathematical models of drug dissolution: a review. *Sch. Acad. J. Pharm*, *3*(5), 388-396.

Sakai, S., Yamada, Y., Yamaguchi, T., Ciach, T., & Kawakami, K. (2009). Surface immobilization of poly (ethyleneimine) and plasmid DNA on electrospun poly (L-lactic acid) fibrous mats using a layer-by-layer approach for gene delivery. *Journal of Biomedical Materials Research Part A: An Official Journal of The Society for Biomaterials, The Japanese Society for Biomaterials, and The Australian Society for Biomaterials and the Korean Society for Biomaterials*, *88*(2), 281-287.

Schiffman, J. D., & Schauer, C. L. (2008). A review: electrospinning of biopolymer nanofibers and their applications. *Polymer reviews*, *48*(2), 317-352.

Schmaljohann, D. (2006). Thermo-and pH-responsive polymers in drug delivery. *Advanced drug delivery reviews*, *58*(15), 1655-1670.

Senapati, S., Mahanta, A. K., Kumar, S., & Maiti, P. (2018). Controlled drug delivery vehicles for cancer treatment and their performance. *Signal transduction and targeted therapy*, *3*(1), 7.

Sharma, A., Gupta, A., Rath, G., Goyal, A., Mathur, R. B., & Dhakate, S. R. (2013). Electrospun composite nanofiber-based transmucosal patch for anti-diabetic drug delivery. *Journal of Materials Chemistry B*, *1*(27), 3410-3418.

Shin, H. J., Lee, C. H., Cho, I. H., Kim, Y. J., Lee, Y. J., Kim, I. A., ... & Shin, J. W. (2006). Electrospun PLGA nanofiber scaffolds for articular cartilage reconstruction: mechanical stability, degradation and cellular responses under mechanical stimulation in vitro. *Journal of Biomaterials Science, Polymer Edition*, *17*(1-2), 103-119.

Singh, S., Pandey, V. K., Tewari, R. P., & Agarwal, V. (2011). Nanoparticle based drug delivery system: advantages and applications. *Indian Journal of Science and Technology*, *4*(3), 177-180.

Slemming-Adamsen, P., Song, J., Dong, M., Besenbacher, F., & Chen, M. (2015). In Situ Cross-Linked PNIPAM/Gelatin Nanofibers for Thermo-Responsive Drug Release. *Macromolecular Materials and Engineering*, *300*(12), 1226-1231.

Song, W., Yu, X., Markel, D. C., Shi, T., & Ren, W. (2013). Coaxial PCL/PVA electrospun nanofibers: osseointegration enhancer and controlled drug release device. *Biofabrication*, *5*(3), 035006.

Taepaiboon, P., Rungsardthong, U., & Supaphol, P. (2006). Drug-loaded electrospun mats of poly (vinyl alcohol) fibres and their release characteristics of four model drugs. *Nanotechnology*, *17*(9), 2317.

Thakkar, S., & Misra, M. (2017). Electrospun polymeric nanofibers: New horizons in drug delivery. *European Journal of Pharmaceutical Sciences*, *107*, 148-167.

Theeuwes, F., & Nelson, T. S. (2004). *U.S. Patent No. 6,726,920*. Washington, DC: U.S. Patent and Trademark Office.

Tipduangta, P., Belton, P., Fabian, L., Wang, L. Y., Tang, H., Eddleston, M., & Qi, S. (2015). Electrospun polymer blend nanofibers for tunable drug delivery: the role of transformative phase separation on controlling the release rate. *Molecular pharmaceutics*, *13*(1), 25-39.

Toomey, P., Kodumudi, K., Weber, A., Kuhn, L., Moore, E., Sarnaik, A. A., & Pilon-Thomas, S. (2013). Intralesional injection of rose bengal induces a systemic tumor-specific immune response in murine models of melanoma and breast cancer. *PloS one*, *8*(7), e68561.

Uhrich, K. E., Cannizzaro, S. M., Langer, R. S., & Shakesheff, K. M. (1999). Polymeric systems for controlled drug release. *Chemical reviews*, *99*(11), 3181-3198.

Wallace, G. G., Higgins, M. J., Moulton, S. E., & Wang, C. (2012). Nanobionics: the impact of nanotechnology on implantable medical bionic devices. *Nanoscale*, *4*(15), 4327-4347.

Wang, B., Wang, Y., Yin, T., & Yu, Q. (2010). Applications of electrospinning technique in drug delivery. *Chemical Engineering Communications*, *197*(10), 1315-1338.

Wang, Y., Kozlovskaya, V., Arcibal, I. G., Cropek, D. M., & Kharlampieva, E. (2013). Highly swellable ultrathin poly (4-vinylpyridine) multilayer hydrogels with pH-triggered surface wettability. *Soft Matter*, *9*(39), 9420-9429.

Wang, Y., Wang, B., Qiao, W., & Yin, T. (2010). A novel controlled release drug delivery system for multiple drugs based on electrospun nanofibers containing nanoparticles. *Journal of pharmaceutical sciences*, *99*(12), 4805-4811.

Wei, M., Gao, Y., Li, X., & Serpe, M. J. (2017). Stimuli-responsive polymers and their applications. *Polymer Chemistry*, *8*(1), 127-143.

Yang, D., Li, Y., & Nie, J. (2007). Preparation of gelatin/PVA nanofibers and their potential application in controlled release of drugs. *Carbohydrate Polymers*, *69*(3), 538-543.

Yoshimoto, H., Shin, Y. M., Terai, H., & Vacanti, J. P. (2003). A biodegradable nanofiber scaffold by electrospinning and its potential for bone tissue engineering. *Biomaterials*, *24*(12), 2077-2082.

Yu, D. G., Zhu, L. M., White, K., & Branford-White, C. (2009). Electrospun nanofiber-based drug delivery systems. *Health*, *1*(02), 67.

Zamani, M., Morshed, M., Varshosaz, J., & Jannesari, M. (2010). Controlled release of metronidazole benzoate from poly ε-caprolactone electrospun nanofibers for periodontal diseases. *European Journal of Pharmaceutics and Biopharmaceutics*, *75*(2), 179-185.

Zamani, M., Prabhakaran, M. P., & Ramakrishna, S. (2013). Advances in drug delivery via electrospun and electrosprayed nanomaterials. *International journal of nanomedicine*, *8*, 2997.

Zelikin, A. N., Ehrhardt, C., & Healy, A. M. (2016). Materials and methods for delivery of biological drugs. *Nature chemistry*, *8*(11), 997.

Zeng, J., Aigner, A., Czubayko, F., Kissel, T., Wendorff, J. H., & Greiner, A. (2005). Poly (vinyl alcohol) nanofibers by electrospinning as a protein delivery system and the retardation of enzyme release by additional polymer coatings. *Biomacromolecules*, *6*(3), 1484-1488.

Zhang, Y., Huang, Z. M., Xu, X., Lim, C. T., & Ramakrishna, S. (2004). Preparation of core−shell structured PCL-r-gelatin bi-component nanofibers by coaxial electrospinning. *Chemistry of Materials*, *16*(18), 3406-3409.

Zhu, Y., Feng, L., Xia, F., Zhai, J., Wan, M., & Jiang, L. (2007). Chemical Dual-Responsive Wettability of Superhydrophobic PANI-PAN Coaxial Nanofibers. *Macromolecular rapid communications*, *28*(10), 1135-1141.

Zupančič, S., Sinha-Ray, S., Sinha-Ray, S., Kristl, J., & Yarin, A. L. (2016). Controlled release of ciprofloxacin from core–shell nanofibers with monolithic or blended core. *Molecular pharmaceutics*, *13*(4), 1393-1404.